博士論文

Human *NBS1* polymorphism reduces DNA repair activity and elevates chromosomal instability

（ヒト *NBS1* の塩基多型は DNA 修復活性を低下させ染色体不安定性を誘起する）

山本　悠貴

Abstract

Failure to expeditiously repair DNA at sites of double-strand breaks (DSB) is an important etiologic factor in cancer development. The Nijmegen breakage syndrome gene (*NBS1*) plays an important role in the cellular response to DSB damage. A rare polymorphic *NBS1* variant that resulted in an isoleucine to-valine substitution at amino acid position 171 (I171V) was first identified in childhood acute lymphoblastic leukemia. This polymorphic variant is located in the N-terminal region that interacts with other DNA repair factors. Previously, a remarkable number of structural chromosomal aberrations in a pediatric aplastic anemia (AA) patient with a homozygous polymorphic variant of NBS1-I171V have been reported; ,however, it was unclear whether this variant affected DSB repair activity or chromosomal instability. In this report, it was demonstrated that *NBS1*-I171V reduces DSB repair activity through a loss of association with the DNA repair factor mediator of DNA-damage checkpoint 1 (MDC1). Further, it was found that heterozygosity in this polymorphic variant was associated with an increased breast cancer risk. In addition, it was shown that this variant exerted a dominant-negative effect on wild-type NBS1, attenuating DSB repair efficiency and elevating chromosomal instability. These findings offer evidence that the failure of DNA repair leading to chromosomal instability has a causal impact on the risk of breast cancer development. Finally, it was found that AZD2281 (a PARP inhibitor) with Bortezomib (26S proteasome inhibitor) inhibited the growth of the cells expressing *NBS1*-I171V and *BRCA1* mutant HCC1937 cells. This result suggested that AZD2281 in combination with Bortezomib effectively inhibited growth of the cancer cells defective in homologous recombination (HR) repair.

Acknowledgements

I first deeply thank my supervisors, Professor Toshiki Watanabe and Associate Professor Hitoshi Satoh for their tremendous efforts, valuable support, and guidance for successful accomplishment of my dissertation.

This study was conducted at the Center for Medical Genomics, National Cancer Center Research Institute. My deepest gratitude also goes to Dr. Tsutomu Ohta for this guidance and support through this study.

I would particularly like to thank Professor Koichi Matsuda (Tokyo University) and Professor Yoichi Furukawa (Tokyo University) for their comments and suggestions.

I would like to thank Dr. Mamiko Miyamoto, Dr. Daisuke Tatsuda (BIKAKEN), Dr. Michiaki Kubo (RIKEN), Dr. Hitoshi Nakagama (National Cancer Center Research Institute), and Professor Yusuke Nakamura (Chicago University) for supporting my experiment.

I would also like to thank Dr. Komatsu (Kyoto University) and Dr. S. Sonobe (Kouchi Medical School, Japan) for courtesy of providing the *NBS1* cDNA, GM07166VA7 cells, and HS-SY-II cells.

I am particularly grateful for the assistance given by all members of the Laboratory of Tumor Cell Biology at Tokyo University.

Finally, I thank my family and my friends for their moral support and warm encouragement.

Contents

Chapter 1

Introduction

1. DNA Repair Factor *NBS1*

1.1. Homologous Recombination Repair

In the natural state, DNA double strand breaks (DSBs) are induced by DNA replication stress and free radicals. DSB often leads to deleterious effects, such as genomic instability. In mammals, the genomic instability changes the quality of genetic information and occasionally initiates carcinogenicity by the activation of oncogenes and/or the inactivation of tumor suppressor genes. Mammalian cells have acquired DSB repair systems to keep the genomic fidelity. The HR repair system is one of such DSB repair systems. It is known that the HR repair system mainly occurs in the S-phase of the cell cycle because it requires intact daughter DNA strands. In the S-phase, DNA polymerase makes newly synthesized DNA with template DNA, and then, two double-strand DNAs (dsDNAs) are located in close proximity to each other. Therefore, if either one of dsDNAs generates DSBs, the DNA makes newly intact DNA with another dsDNA. This is also referred to as an error-free DSB repair system.

Gene products of *MRE11*, *RAD50*, and *NBS1* make the MRE11/RAD50/NBS1 protein complex (MRN complex), which is involved in the early steps of the HR repair pathway (1). In early steps of this pathway, ataxia telangiectasia-mutated (ATM) kinase, a member of the phosphatidylinositol 3-kinase-related kinase (PIKK) family of serine/threonine protein kinases, accumulates at the sites of DSBs. ATM phosphorylates H2A histone family member X (H2AX) on Serine 139 (also known as γH2AX) (2) (Fig. 1 [Ⅱ]). γH2AX recruits mediator of DNA damage checkpoint 1 (MDC1) to the sites of DSBs (Fig. 1 [Ⅲ]). MDC1 recruits the MRN complex to the site of the DSBs (3, 4) (Fig. 1 [Ⅳ]). The MRN complex initiates resection of the DSB ends to creates single-stranded 3'-overhangs (5) (Fig.2 [Ⅵ]). The MRN recruits CtBP-interacting protein (CtIP) to the site

of DSBs (6) (Fig. 2 [Ⅶ]). CtIP creates long single-stranded 3'-overhangs (7) (Fig. 2 [Ⅷ]). The MRN complex recruits replication protein A (RPA) containing phosphorylated RPA32 to single-stranded 3'-overhangs. (8) (Fig.2 [Ⅸ]). In addition, CtIP interacts with Breast cancer type 1 susceptibility protein (BRCA1) (6). BRCA1 apparently plays a role in downstream HR repair system by promoting the accumulation of downstream HR repair factors. BRCA1 recruits breast cancer type 2 susceptibility protein (BRCA2) to single-stranded 3'-overhangs through partner and localizer of BRCA2 (PALB2) (9) (Fig. 3 [Ⅹ]). BRCA2 supports RAD51 loading onto single-stranded 3'-overhangs in combination with phosphorylated RPA32 (10) (Fig. 3 [Ⅹ Ⅰ]). RAD51 is associated with the strand exchange step of HR repair (11). 3'-ssDNA then invades daughter DNA strands with the strand exchange ability of RAD51 (Fig. 3 [Ⅹ Ⅱ]). Finally, DNA polymerase synthesizes a new DNA strand with the complemental DNA strands as mold (Fig. 3 [Ⅹ Ⅲ]), and DNA ligase attaches the newly synthesized DNA ends to the DNA injured with DSB (Fig. 3 [Ⅹ Ⅳ]).

1.2. Finding DNA Repair Factor *NBS1*

NBS1 was identified as the causative gene of Nijmegen breakage syndrome, which is an autosomal recessive human disease, and the clinical features of this syndrome include growth retardation, immunodeficiency, and increased susceptibility to malignancies (12). A gene product of *NBS1* is a protein involved in the Nijmegen breakage syndrome 1 (NBS1), which is involved in the repair of DSB in DNA (13). It has been reported that in

a mouse model, the null mutation of *Nbn*, the mouse homolog of the *NBS1* gene, caused mouse embryonic lethality, but heterozygous knockout ($Nbn^{+/-}$) mice developed the lymphoma tumors, some types of adenomas, and carcinomas (14, 15). For these studies it has been considered that the DNA repair factor NBS1 is associated with cancer.

1.3 Functions of NBS1 in DNA Repair

DNA repair factor NBS1 is a member of the MRE11/RAD50/NBS1 (MRN) protein complex, which is involved in the repair of DSB in DNA (13). NBS1 consists of some functional regions (Fig. 4). Its C-terminal region contains binding motif of MRE11 and ATM (16–18), whereas its N-terminal region contains forkhead-associated (FHA) and breast cancer C-terminal (BRCT) domains that mediate phospho-dependent protein - protein interactions (19–21). NBS1 binds to CtIP through the FHA domain, leading to subsequent DNA end resection during HR repair (when CtIP is phosphorylated on threonine [22]). As previously described, NBS1 is mainly associated with the HR repair system and recruits MRE11/RAD50 to the DSB site and is accumulated by the interaction with MDC1. In this step, NBS1 interacts MDC1 with the FHA and BRCT domains of NBS1 and the serine-aspartic acid-threonine (SDT) motif of MDC1 (21–23).

In the DSB repair system, NBS1 is related to the cell cycle checkpoint, which is mainly the intra-S-phase checkpoint. It has been considered that the cell cycle NBS1 checkpoints consist of three parallel pathways. The first pathway is the ATM /NBS1/ CHK2 pathway. NBS1 is associated with the activation of ATM and CHK2 (18, 24, 25). ATM, which is activated by NBS1, activates CHK2, and then, the activated CHK2 phosphorylates CDC25A (26). The phosphorylated CDC25A phosphorylates CDK2, and this leads to a disruption of CDK2, which finally causes the intra-S-phase checkpoint

(26).

The second pathway is the ATM/NBS1/SMC1 pathway. In this pathway, NBS1 is required for recruitment of ATM to damaged DNA sites, and this leads to phosphorylation of SMC1, which activates the intra-S-phase checkpoint (27).

The third pathway is the ATM/NBS1/FANCD2 pathway. In this pathway, ATM phosphorylates FANCD2, and this phosphorylation is required for the phosphorylation of NBS1 by ATM, and it leads to intra-S-phase checkpoint (28, 29).

1.4 *NBS1* Polymorphisms and Mutations

In previous studies, it has been considered that the DNA repair factor NBS1 is associated with cancer. Hence, the correlation between carriers of NBS1 gene mutations and the development of tumors have been researched. The *NBS1* mutation of the protein associated with the Nijmegen breakage syndrome mainly has a five-base deletion from the six hundred and fifty-seventh base (657 del 5) (30). Thus heterozygous 657del5 mutation was observed in the stomach, colorectal, melanoma, NHL, and breast cancers (31, 32).

In addition, heterozygous 643C>T(R215W) polymorphism was observed in the patient of colorectal cancer and acute lymphoblastic leukemia (ALL) (32).

A rare polymorphic *NBS1* variant (511A>G) that resulted in an isoleucine-to-valine substitution at amino acid position 171 (I171V) was first identified in childhood ALL (33). The *NBS1*-I171V polymorphic variant is located in the BRCT domain, which is highly conserved in humans, mice, rats, chickens, and African clawed frogs (Fig. 4). It has previously been reported that aplastic anemia in a Japanese child with a homozygous polymorphic variant of NBS1-I171V has been detected (34). Thus, the chromosomes of

the lymphoblastic cell lines derived from this patient contained a remarkable number of structural chromosomal aberrations and reduced DSB repair activity (34). Furthermore, the I171V rare polymorphic variant was frequently detected in patients with breast, head and neck, and colorectal cancer risks (35–38).

1.5 Problems Need to be Solved

As previously described, the polymorphism of NBS1 is considered to be associated with the risk of cancer (32–38). However, the precise molecular mechanisms associated with the risk of cancer are not well known. It is noteworthy that the heterozygous *NBS1*-I171V polymorphism is higher in some cancers than in population controls. In addition, the homozygous *NBS1*-I171V polymorphism was observed in aplastic anemia patients, and the chromosomes of the lymphoblastic cell lines derived from this patient had chromosomal instability, which is frequently found in cancer cells. Based on these results, it has been considered that NBS1 amino acid position 171 is important for the function of NBS1. Hence, the molecular mechanisms of the *NBS1*-I171V polymorphic variant in the DSB repair activity were analyzed.

Furthermore, the medicine with HR repair pathway, that does not lead to greater side effects in normal cells, such as PARP1 inhibitor, was found in meager quantities (39, 40). Therefore I searched for effective inhibitors to reduce the growth of HR repair-deficient cells.

Chapter 2

Materials and Methods

2.1 Cell Lines

HeLa　and HCC1937 cells were obtained from the American Type Culture Collection (ATCC). GM07166VA7 and GM07166VA7 transfected with DR-GFP reporter cells were obtained from Dr. K. Komatsu (Kyoto University). HS-SY-II cells were obtained from Dr. S. Sonobe (Kouchi Medical School).

2.2 Antibodies

The following commercially available antibodies were used: mouse anti-FLAG M2 monoclonal antibody (Sigma-Aldrich), rabbit anti-MDC1 antibody, mouse anti-MDC1 antibody, rabbit anti-p95 NBS1 antibody, rabbit anti-Mre11 antibody (Abcam), rabbit anti-phospho RPA32 (S4/S8) antibody (Bethyl Laboratories), mouse anti-phospho histone H2AX (Ser139) (Upstate), rabbit anti-RAD50 antibody, rabbit anti-RAD51 antibody (Santa Cruz Biotechnology) and rabbit anti-BRCA1 antibody (Merck Millipore).

2.3 Plasmids and Stable Cell Lines

The plasmids of pDRGFP and pCBASceI were purchased from addgene. The full-length human *NBS1* cDNA was a gift from Dr. Komatsu. The cDNA of *NBS1*-I171V or *NBS1*-WT with a 3xFlag-His6-HA-tag at C-terminus was generated by using PCR and then ligated into the pEB-Multi-Neo mammalian expression vector (Wako). These vectors were transfected into GM07166VA7 cells, GM07166VA7 cells containing DR-GFP reporter and HeLa cells. The cells were cultured in the presence of 600 or 800 μg/ml G418 (Calbiochem) for 2 weeks, after which clones were isolated and selected on the basis of their NBS1 expression. The selected clones expressed equivalent levels of protein.

2.4 Immunoprecipitation

For immunoprecipitation analysis, the cells were washed with phosphate-buffered saline (PBS) and sonicated in lysis buffer (150 mmol/L NaCl, 20 mmol/L Tris-HCl [pH 7.9], 20% glycerol, and 1 mmol/L Pefabloc [a protease inhibitor; Roche]). The lysate (1 mg) was mixed with anti-Flag M2 Affinity Gel (Sigma-Aldrich) and incubated for 4 hours at 4°C. The gel was washed 3 times with lysis buffer. The immunoprecipitated proteins were separated by using sodium dodecyl sulfate polyacrylamide gel electrophoresis (SDS-PAGE) and then incubated with the indicated antibodies.

2.5 Immunofluorescence

For immunofluorescence analysis, the cells were cultured on glass coverslips, exposed to 10 Gy of ionizing radiation (IR). After 4 hours, the cells were fixed in ice-cold 4% paraformaldehyde for 1 hour, permeabilized with 0.1% TritonX-100 at room temperature, immersed in blocking reagent (2% Normal Swine Serum [Funakoshi], 0.05% TritonX-100) for 30 minutes at room temperature, and then incubated with the indicated primary antibodies overnight at 4°C. The cells were incubated with secondary antibodies conjugated to Alexa Fluor 488 or Alexa Fluor 555 (Invitrogen) for 1 hour at room temperature and stained with 2 μg/ml of 4',6- diamidino-2-phenylindole dihydrochloride (DAPI) for 10 minutes at room temperature. Images were captured with a confocal laser microscope (Carl Zeiss) with a 40x water immersion objective.

2.6 Cell Survival Assay

An appropriate number of cells was plated and then exposed to IR, mitomycin C (MMC), a poly-(ADP-ribose) polymerase 1 (PARP1) inhibitor (AZD2281) and Bortezomib. After 10 days of incubation, the surviving fractions were calculated by counting the number of colonies.

2.7 Flow Cytometry

For DNA content analysis, an appropriate number of cells was plated and then exposed to 10 Gy of IR. After 6 hours, the cells were collected and fixed with ice-cold 70% EtOH for 30 minutes. The cells were incubated with PBS containing 0.2 mg/mL of RNase A at 37 ℃ for 10 minutes and then incubated with PBS containing 1mM of EDTA and 10 μg/mL of propidium iodide for 30 minutes at 4 ℃ in the dark. All samples were analyzed using a flow cytometer EC800 (Sony Biotechnology) and EC800 software.

2.8 Cytogenetic Analysis

After exposure to IR, the cells were cultured for 3 days and then treated with colcemid (0.02 μg/ml) for 2 hours before being harvested. Chromosome slides were prepared by using standard protocols and then stained with a 5% Giemsa solution (Wako) for 30 minutes. For each cell line, about 1,600 well-spread metaphase chromosomes were screened for structural chromosomal aberrations. *P* values were calculated by using the chi-square test.

2.9 Sample Collection, Genotyping, and Statistical Analysis

I obtained DNA samples of 1,524 breast cancer cases and 1,462 controls from the

Biobank Japan Project as described previously (PMID: 22951594). As part of this project, patients' DNA samples were collected through a collaborative network of 66 hospitals throughout Japan. A list of participating hospitals can be found at the following website: http://biobankjp.org/plan/member_hospital.html. Genotyping of the *NBS1* variations at amino acid position 171 was performed by direct sequencing. The primers used for amplification were as follows: forward, 5'-TGGATGTAAACAGCCTCTTTGT-3'; reverse, 5'-TGAAACAAGCATTAAAGAGGGAA-3'. The odds ratios (OR) were calculated in a dominant mode. *P* values were calculated by using the chi-square test.

2.10 HR Reporter Assay

GM07166VA7 cells containing DR-GFP reporter were given from Dr. Komatsu and I prepared the cell line transfected cDNA of *NBS1* as described in Chapter 2.3. Homologous recombination (HR) repair frequency in the cell lines using DR-GFP system was performed as described previously (41, 42).

Chapter 3

Results

3.1 *NBS1*-I171V Polymorphic Variant and Risk of Cancer

3.1.1 *NBS1*-I171V Polymorphic Variant Reduced DSB Repair Activity

To explore the biological consequences of the NBS1-I171V substitution, the cell lines that express the polymorphic variants of the *NBS1* gene were prepared. First, expression vectors of the *NBS1* cDNA that encodes a protein with either isoleucine (NBS1-WT) or valine (NBS1-I171V) at amino acid position 171 were constructed. The vectors were stably transfected into NBS1-deficient GM07166VA7 cells, which were established from a patient with Nijmegen breakage syndrome. The GM07166VA7 cells had a homozygous 657del5 mutation in exon 6 and hardly expressed truncated NBS1. Clones with equivalent levels of *NBS1* expression were isolated and selected for further analysis (Fig. 5).

These NBS1-expressing cell lines were used to assess cell survival in response to DNA damage caused by ionizing radiation (IR) or the cross-linking agent mitomycin C (MMC). An analysis of cell survival revealed that the cell line expressing NBS1-I171V was more sensitive to IR and MMC than was the cell line expressing NBS1-WT (Fig. 6). Next, the HR repair frequency in these NBS1-expressing cell lines with DR-GFP system was analyzed (41, 42). When *Sce* I expression was induced, the cell line expressing NBS1-I171V showed a three-fold lower frequency in HR repair compared with that of the cell line expressing NBS1-WT (Fig. 7).

3.1.2 *NBS1*-I171V Polymorphic Variant Decreased the Localization of the MRN Complex to Sites of DSB

Immunoprecipitation analysis in the cell lines indicated that both NBS1-I171V and NBS1-WT bound to MRE11 and RAD50 (Fig. 8), suggesting that NBS1-I171V can be

incorporated into the MRN protein complex. NBS1 is known to be involved in an early step of DSB repair. Immunofluorescence was used to examine whether NBS1-I171V localized to sites of DSB in cells exposed to IR. NBS1 foci in cells expressing NBS1-WT but not in those expressing NBS1-I171V were observed (Fig. 9A and 9B). MRE11 foci were also identified in cells expressing NBS1-WT, but not in those expressing NBS1-I171V (Fig. 9C and 9D). γH2AX foci were identified in both the cells expressing NBS1-I171V and those expressing NBS1-WT, where they colocalized with the NBS1-WT or MRE11 foci (Fig. 9). These results suggest that after exposure to IR, the localization of NBS1-I171V to DSB sites may be less prominent than that of NBS1-WT.

3.1.3 *NBS1*-I171V Polymorphic Variant Reduced DSB Repair Activity Through Loss of Association with MDC1

Because MDC1 recruits NBS1 to sites of DSB after the IR treatment (3, 4), its localization in cells that had been exposed to IR was examined. MDC1 foci were identified at sites of DSB in cells expressing either NBS1-I171V or NBS1-WT (Fig. 10A and 10B). Next, the interaction between NBS1-I171V and MDC1 was characterized by conducting an immunoprecipitation analysis. After exposure to IR, a large amount of MDC1 coprecipitated with NBS1-WT, but not with NBS1-I171V (Fig. 11A). It was also determined that MDC1 foci localized at sites of DSB with NBS1-WT foci but not with NBS1-I171V foci after the IR treatment (Fig. 11B and C).

3.1.4 Intra-S-Phase Cell Cycle Arrest is Failed in *NBS1*-I171V Polymorphic Variant

It was reported that NBS cells exposed to IR showed an abnormal cell cycle (43). Therefore, the cell-cycle status of the cells that had been exposed to IR was examined. It

was observed that the ratio of the S phase in the cell expressing the NBS1-WT was increased by IR treatment but not in the cells expressing the NBS1-I171V or the vector (Fig. 12).

3.1.5 *NBS1*-I171V Polymorphic Variant Increases Risk of Breast Cancer

To date, the *NBS1*-I171V polymorphic variant was detected frequently only in Polish patients with breast, head and neck, and colorectal cancers (35–38). However, other groups did not find a similar association in European patients with breast cancer, leukemia, or lymphoma (44–46). It remains unclear whether this particular polymorphic variant of the *NBS1* gene is associated with cancer. As previously described, although null mutations in the mouse *NBS1* gene resulted in embryonic lethality at the blastocyst stage, heterozygous knockout ($NBS1^{+/-}$) mice developed a wide array of tumors. Moreover, cell cycle-dependent association of BRCA1 with the MRN protein complex contributed to the activation of HR-mediated DSB repair in S and G2 phases of the cell cycle (6). These results strongly suggest that the *NBS1*-I171V polymorphic variant may increase breast cancer risk. Therefore, the association of the *NBS1*-I171V polymorphic variant with breast cancer in a Japanese population was analyzed. Only seven women (0.48%) with the heterozygous polymorphic variant were found in the control group (n= 1462). None of the patients in the breast cancer or control groups carried the homozygous polymorphic variant of the *NBS1*-I171V substitution. The frequency of patients with the heterozygous *NBS1* polymorphic variant in the Japanese breast cancer group [odds ratio (OR) = 3.19, 95% confidence interval (CI) = 1.36–7.44, $P = 0.0048$] was significantly higher than that in the control group (Table 1).

3.1.6 *NBS1*-I171V Polymorphic Variant Exerts a Dominant-Negative Effect on the Function of NBS1-WT

The previously described finding appears to suggest that NBS1-I171V exerts a dominant-negative effect on the function of NBS1-WT. To test this hypothesis, HeLa cells expressing NBS1-I171V, which also express endogenous NBS1, were prepared. Clones were isolated and selected on the basis of their exogenous and endogenous NBS1 expressions, with the selected clones expressing equivalent levels of protein (Fig. 13A). Next, the cell survival in response to DNA damage caused by exposure to IR or MMC was assessed. The cell line expressing NBS1-I171V was more sensitive to IR and MMC than the cell line expressing NBS1-WT or vector (Fig. 13B).

Next, immunofluorescence was used to examine whether NBS1- I171V localizes to DSB sites in HeLa cells expressing NBS1-I171V exposed to IR. The cell line expressing NBS1-I171V showed a twofold lower focus counts of NBS1 compared with those of the cell line expressing NBS1-WT or the vector was observed (Fig. 11A and B). MDC1 localization in cells that had been exposed to IR was examined. MDC1 foci were identified at sites of DSB in cells expressing either NBS1-I171V or NBS1-WT (Fig. 15A and B). This result suggests that MDC1's ability to localize to the sites of DSB after IR treatment is unaffected by the NBS1-I171V. It was observed that NBS1-I171V foci localized at sites of MDC1 foci were decreased after IR treatment (Fig. 15C and D). Next, I analyzed the localization of MRE11, phosphorylated RPA32, RAD51, or BRCA1 in IR-exposed cells. The cell line expressing NBS1-I171V showed a two- to threefold lower focus counts of MRE11, phosphorylated RPA32, RAD51 or BRCA1 compared with the cell line expressing NBS1-WT or the vector (Figs. 14C and D, 16 and 17). These results suggest that this variant exerted a dominant-negative effect on wild-type NBS1.

3.1.7 *NBS1*-I171V Polymorphic Variant Elevated Chromosomal Instability

It was reported that a remarkable number of structural chromosomal aberrations were identified in lymphoblastic cell lines derived from a pediatric aplastic anemia (AA) patient with a homozygous polymorphic variant of NBS1-I171V (34). However, it was unclear whether this variant affected chromosomal instability. Therefore, the structural aberrations of the chromosomes in each cell line after exposure to IR were assessed, and it was observed that the number of aberrations in the cell line expressing NBS1-I171V (28 double minutes [DMs], seven chromatid gaps [CTGs], and eight chromatid breaks [CTBs] / ~ 1,600 chromosomes; a representative metaphase spread is shown in Fig. 18) was significantly higher than that of cell line expressing either NBS1-WT or the vector control (NBS1-WT: four DMs and four CTGs, vector control: four DMs, one CTG, and one CTB; both / ~ 1,600 chromosomes; Fig. 18).

3.2 Chemotherapy for Cells Reduced Activity of HR Repair

3.2.1 Cells Reduced Activity of HR Repair were Sensitive to PARP1 Inhibitor and Proteasome Inhibitor

It has been previously reported that a PARP1 inhibitor reduced the growth of HR repair–deficient cells (39, 40). Therefore, cell survival in response to the PARP1 inhibitor (AZD2281, also known as Olaparib) was examined. An analysis of cell survival revealed that the cell line expressing NBS1-I171V and vector control were more sensitive to AZD2281 than the cell line expressing NBS1-WT (Fig. 19A). When cell survival in response to several reagents was examined, it was found that the cell lines expressing NBS1-I171V and vector control were more sensitive to Bortezomib (26S proteasome inhibitor) than the cell line expressing NBS1-WT was (Fig. 19B). These results suggest

that Bortezomib may reduce growth of HR repair–deficient cells, such as BRCA1- and BRCA2- mutated cells. Therefore, the survival of HCC1937 cells, which have homozygous mutation in *BRCA1* gene (insertion C at nucleotide 5382), was examined in response to Bortezomib. Similar to the cell line expressing NBS1-I171V, HCC1937 cells were more sensitive to Bortezomib than GM07166VA7cells expressing NBS1-WT (Fig. 21A).

Next, cell survival in response to AZD2281 with Bortezomib was examined. Growth inhibition of the cell line expressing NBS1-I171V and vector control that had been exposed to AZD2281 with Bortezomib was observed (Fig. 20). Growth inhibition of HCC1937 cells that had been exposed to AZD2281 with Bortezomib was also observed (Fig. 21B).

Chapter 4

Discussions

4.1 *NBS1*-I171V Polymorphic Variant Reduces HR Repair Activity with Loss of Interaction of MDC1

A large amount of MDC1 coprecipitated with NBS1-WT but not with NBS1-I171V after IR exposure was observed (Fig. 11A). This results is consistent with the reports that both FHA and BRCT domains in NBS1 are important for its association with MDC1 (21,22). The NBS1-K160M mutant, which resulted in an lysine to methionine substitution at amino acid position 160 within the BRCT domain, appears to reduce its binding activity to MDC1 (21). Therefore, it seems that the NBS1-I171V mutant within the BRCT domain affects a structure of the BRCT domain and abolishes the interaction between NBS1 and MDC1.

It was shown that NBS1-I171V decreased the localization of the MRN complex to sites of plural DSBs through loss of association with MDC1 (Fig. 9). The MRN complex appears to initiate resection of the DSB ends to create single-stranded 3'-overhangs that can be repaired by the HR system. In addition, the complex recruits RPA32, to single-stranded DNA at sites of DSB. The production of single-stranded DNA at the ends of DSB using immunofluorescence to analyze the localization of phosphorylated RPA32 in cells exposed to IR was examined. Phosphorylated RPA32 foci were identified at DSB sites in cells expressing NBS1-WT but not in those expressing NBS1-I171V or the vector control (Fig. 22A and B). It was reported that BRCA1 also promoted the induction of the single-stranded DNAs at DSB sites. Therefore, the BRCA1 localization in cells that had been exposed to IR was examined. BRCA1 foci were identified at DSB sites in cells expressing NBS1-WT but not in those expressing NBS1-I171V or the vector (Fig.23A and B). Because RAD51 also was recruited to the single-stranded 3'-overhangs after the IR

treatment, RAD51 localization in cells that had been exposed to IR was examined. RAD51 foci were identified at sites of DSB in cells expressing NBS1-WT, but not in those expressing NBS1-I171V or the vector (Fig. 23C and D). These results are consistent with my findings that the localization of NBS1-I171V to sites of IR-induced DSB was less pronounced than that of NBS1-WT (Fig. 9A and B), and suggest that NBS1-I171V decreases the localizations of the MRN complex and BRCA1 to DSB sites. These aberrant localizations appear to result in decreased production of repairable single-stranded DNA and reduced DSB repair activity.

4.2 *NBS1*-I171V Polymorphic Variant Increases Risk of Breast Cancer

It was observed that the frequency of patients with the heterozygous *NBS1* polymorphic variant in the Japanese breast cancer group was threefold higher than that in the control group. This result suggests that the *NBS1*-I171V variant increases the risk of breast cancer in Japanese women. None of the patients in the breast cancer or control group carried the homozygous polymorphic variant of the *NBS1*-I171V substitution. However, aplastic anemia (AA) in a Japanese child with a homozygous polymorphic variant of *NBS1*-I171V was reportedly detected(34). This report suggests that the people with the homozygous polymorphic variant of the *NBS1*-I171V are born at low frequency.

4.3 *NBS1*-I171V Polymorphic Variant Exerts a Dominant-Negative Effect on the Function of NBS1-WT and Elevates Chromosomal Instability

Fig. 13 showed that the total amount of NBS1 protein in a HeLa cell line expressing NBS1-I171V or NBS1-WT was almost the same as that in a HeLa cell line expressing a

vector. Because NBS1-I171V incorporates into the MRN protein complex (Fig. 8), half of the MRN protein complex contains NBS1-I171V in a HeLa cell line expressing NBS1-I171V. These results suggest that decreased amounts of MRN protein complex containing wild-type NBS1 in HeLa cell line expressing NBS1-I171V may show a dominant-negative effect in response to DNA damage caused by IR or MMC exposure (Fig. 13-17)

It was observed that chromosomal instability was elevated in cells expressing NBS1-I171V because its dominant-negative effects on endogenous NBS1 reduced DSB repair. This result is consistent with those of previous findings that postulate that the chromosomes of lymphoblastic cell lines derived from the patient's father carrying the heterozygous polymorphic variant of the *NBS1*-I171V substitution contain a remarkable number of structural chromosomal aberrations (34). These results suggest that the NBS1-I171V polymorphic variant is associated with cancer development.

4.4 AZD2281 and Bortezomib reduce the growth of HR deficient cells.

It was found that the cell line expressing NBS1-I171V was more sensitive to AZD2281 or Bortezomib than was the cell line expressing NBS1-WT; however, it was more resistant to AZD2281 or Bortezomib than was the cell line expressing a vector in Fig. 19. These results indicated that damage by AZD2281 or Bortezomib was different from that caused by IR or MMC (Fig. 6). It was shown that the HR repair activity of GM07166VA7 cells expressing NBS1-I171V was almost similar to that of GM07166VA7 cells expressing a vector in Fig. 7. These results suggested that damage caused by AZD2281 or Bortezomib was repaired by both HR repair-dependent and -independent mechanisms. It was suggested that NBS1-I171V has the independent HR-repair activity to repair a part of the damage caused by AZD2281 or Bortezomib. However, the activity of NBS1-

I171V and the damage caused by Bortezomib are still unclear. Thus, further research on NBS1-I171V function and the damage caused by Bortezomib is necessary.

Growth inhibition of the cell line expressing NBS1-I171V and vector control and of the HCC1937 cells (BRCA1 mutant cells) that had been exposed to AZD2281 with Bortezomib (Fig. 20 and 21) was observed. These results suggest that AZD2281 in combination with Bortezomib provided effective growth inhibition of the cancer cells defective in HR repair.

References

1. Carney JP, Maser RS, Olivares H, Davis EM, Le Beau M, Yates JR 3rd, et al. The hMre11/hRad50 protein complex and Nijmegen breakage syndrome: linkage of double-strand break repair to the cellular DNA damage response. Cell 1998; 93: 477-86.

2. Burma S, Chen BP, Murphy M, Kurimasa A and Chen DJ. ATM phosphorylates histone H2AX in response to DNA double-strand breaks. J Biol Chem 2001; 276, 42462-7.

3. Goldberg M, Stucki M, Falck J, D'Amours D, Rahman D, Pappin D, et al. MDC1 is required for the intra-S-phase DNA damage checkpoint. Nature 2003; 421: 952-6.

4. Stewart GS, Wang B, Bignell CR, Taylor AM and Elledge SJ. MDC1 is a mediator of the mammalian DNA damage checkpoint. Nature 2003; 421: 961-6.

5. Kelly MT, Shyng-Shiou FY, Eva YHPL and Patrick S. Nuclease activities in a complex of human recombination and DNA repair factors Rad50, Mre11, and p95. J Biol Chem 1998; 273: 21447-50.

6. Chen L, Nievera CJ, Lee AY and Wu X. Cell cycle-dependent complex formation of BRCA1.CtIP.MRN is important for DNA double-strand break repair. J Biol Chem 2008; 283: 7713-20.

7. Sartori AA, Lukas C, Coates J, Mistrik M, Fu S, Bartek J, et al. Human CtIP promotes DNA end resection. Nature 2007; 450: 509-14.

8. Robison JG, Lu L, Dixon K and Bissler JJ. DNA lesion-specific co-localization of the Mre11/Rad50/Nbs1 (MRN) complex and replication protein A (RPA) to repair foci. J Biol Chem 2005; 280: 12927-34.

9. Shirley MHS, Michael SYH and Junjie C. PALB2 is an integral component of the BRCA complex required for homologous recombination repair. Proc Natl Acad Sci U S A 2009; 106: 155-60.

10. Liu J, Doty T, Gibson B and Heyer WD. Human BRCA2 protein promotes RAD51 filament formation on RPA-covered single-strand DNA. Nat Struct Mol Biol 2010; 17: 1260-

2.

11. Sung P and Robberson DL. DNA strand exchange mediated by a RAD51-ssDNA nucleoprotein filament with polarity opposite to that of RecA. Cell 1995; 82: 453–61.

12. Weemaes CM, Hustinx TW, Scheres JM, van Munster PJ, Bakkeren JA, Taalman RD. A new chromosomal instability disorder: the Nijmegen breakage syndrome. Acta Paediatr Scand 1981; 70: 557-64.

13. Carney JP, Maser RS, Olivares H, Davis EM, Le Beau M, Yates JR 3rd, et al. The hMre11/hRad50 protein complex and Nijmegen breakage syndrome: linkage of double-strand break repair to the cellular DNA damage response. Cell 1998; 93: 477-86.

14. Demuth I, Frappart PO, Hildebrand G, Melchers A, Lobitz S, Stöckl L, et al. An inducible null mutant murine model of Nijmegen breakage syndrome proves the essential function of NBS1 in chromosomal stability and cell viability. Hum Mol Genet 2004; 13: 2385-97.

15. Dumon-Jones V, Frappart PO, Tong WM, Sajithal G, Hulla W, et al. Nbn heterozygosity renders mice susceptible to tumor formation and ionizing radiation-induced tumorigenesis. Cancer Res. 2003; 63: 7263-9.

16. Desai-Mehta A, Cerosaletti KM, Concannon P. Distinct functional domains of nibrin mediate Mre11 binding, focus formation, and nuclear localization. Mol Cell Biol 2001; 21: 2184-91.

17. Falck J, Coates J, Jackson SP. Conserved modes of recruitment of ATM, ATR and DNA-PKcs to sites of DNA damage. Nature 2005; 434: 605-11.

18. You Z, Chahwan C, Bailis J, Hunter T, Russell P. ATM activation and its recruitment to damaged DNA require binding to the C terminus of Nbs1. Mol Cell Biol 2005; 25: 5363-79.

19. Kobayashi J, Tauchi H, Sakamoto S, Nakamura A, Morishima K, Matsuura S, et al. NBS1 localizes to gamma-H2AX foci through interaction with the FHA/BRCT domain. Curr Biol 2002; 12: 1846-51.

20. Chapman JR, Jackson SP. Phospho-dependent interactions between NBS1 and MDC1 mediate chromatin retention of the MRN complex at sites of DNA damage. EMBO Rep 2008; 9: 795-801.

21. Lloyd J, Chapman JR, Clapperton JA, Haire LF, Hartsuiker E, Li J, et al. A supramodular FHA/BRCT-repeat architecture mediates Nbs1 adaptor function in response to DNA damage. Cell 2009; 139: 100-11.

22. Williams RS, Dodson GE, Limbo O, Yamada Y, Williams JS, Guenther G, et al. NBS1 flexibly tethers Ctp1 and Mre11-Rad50 to coordinate DNA double-strand break processing and repair. Cell 2009; 139: 87-99.

23. Melander F, Bekker-Jensen S, Falck J, Bartek J, Mailand N and Lukas J. Phosphorylation of SDT repeats in the MDC1 N terminus triggers retention of NBS1 at the DNA damage-modified chromatin. J Cell Biol 2008; 181: 213-26.

24. Lim DS, Kim ST, Xu B, Maser RS, Lin J, Petrini JH, et al. ATM phosphorylates p95/nbs1 in an S-phase checkpoint pathway. Nature 2000; 404: 613-7.

25. Buscemi G, Savio C, Zannini L, Micciche F, Masnada D, Nakanishi M, et al. Chk2 activation dependence on Nbs1 after DNA damage. Mol Cell Biol 2001; 21: 5214-22.

26. Jacob F, Niels M, Randi GS, Jiri B and Jiri Lukas. The ATM-Chk2-Cdc25A checkpoint pathway guards against radioresistant DNA synthesis. Nature 2001; 410: 842-7.

27. Kitagawa R, Bakkenist CJ, McKinon PJ and Kastan MB. Phosphorylation of SMC1 is a critical downstream event in the ATM-NBS1-BRCA1 pathway. Genes Dev 2004; 18: 1423-38.

28. Nakanishi K, Taniguchi T, Ranganathan V, New HV, Moreau LA, Stotsky M, et al. Interaction of FANCD2 and NBS1 in the DNA damage response. Nat Cell Biol 2002; 4: 913-20.

29. Toshiyasu T, Irene GH, Bo X, Paul RA, Richard CG, Seong-Tae K, et al. Convergence of the Fanconi anemia and ataxia telangiectasia signaling pathways. Cell 2002; 109: 459-72.

30. Varon R, Vissinga C, Platzer M, Cerosaletti KM, Chrzanowska KH, Saar K, et al. Nibrin, a novel DNA double-strand break repair protein, is mutated in Nijmegen breakage syndrome. Cell 1998; 93: 467-76.

31. Seemanova E, Jarolim P, Seeman P, Varon R, Digweed M, Swift M, et al. Cancer risk of heterozygotes with the NBN founder mutation. J Natl Cancer Inst 2007; 99: 1875-80.

32. Steffen J, Varon R, Mosor M, Maneva G, Maurer M, Stumm M, et al. Increased cancer risk of heterozygotes with NBS1 germline mutations in Poland. Int J Cancer 2004; 111: 67-71.

33. Varon R, Reis A, Henze G, von Einsiedel HG, Sperling K, Seeger K. Mutations in the Nijmegen Breakage Syndrome gene (NBS1) in childhood acute lymphoblastic leukemia (ALL). Cancer Res 2001; 61: 3570–2.

34. Shimada H, Shimizu K, Mimaki S, Sakiyama T, Mori, T, Shimasaki N, et al. First case of aplastic anemia in a Japanese child with a homozygous missense mutation in the NBS1 gene (I171V) associated with genomic instability. Hum Genet 2004; 115: 372-6.

35. Mosor M, Ziółkowska I, Pernak-Schwarz M, Januszkiewicz-Lewandowska D, Nowak J. Association of the heterozygous germline I171V mutation of the NBS1 gene with childhood acute lymphoblastic leukemia. Leukemia 2006; 20: 1454–6.

36. Rozonowski K, Januszkiewicz-Lewandowska D, Mosor M, Pernak M, Litwiniuk M, Nowak J. I171V germline mutation in the NBS1 gene significantly increases risk of breast cancer. Breast Cancer Res Treat 2008; 110: 343–8.

37. Ziolkowska I, Mosor M, Wierzbicka M, Rydzanicz M, Pernak-Schwarz M, Nowak J. Increased risk of larynx cancer in heterozygous carriers of the I171V mutation of the NBS1 gene. Cancer Sci 2007; 98: 1701–5.

38. Nowak J, Mosor M, Ziółkowska I, Wierzbicka M, Pernak-Schwarz M, Przyborska M, et al. Heterozygous carriers of the I171V mutation of the NBS1 gene have a significantly increased risk of solid malignant tumours. Eur J Cancer 2008; 44: 627–30.

39. Farmer H, McCabe N, Lord CJ, Tutt AN, Johnson DA, Richardson TB, et al. Targeting the DNA repair defect in BRCA mutant cells as a therapeutic strategy. Nature 2005; 434: 917-21.

40. Bryant HE, Schultz N, Thomas HD, Parker KM,Flower D, Lopez E, et al. Specific killing of BRCA2-deficient tumors with inhibitors of poly(ADP-ribose) polymerase. Nature 2005; 434: 913-7.

41. Pierce AJ, Johnson RD, Thompson LH, Jasin M. XRCC3 promotes homology-directed repair of DNA damage in mammalian cells. Genes Dev 1999; 13:2633-8.

42. Sakamoto S, Iijima K, Mochizuki D, Nakamura K, Teshigawara K, Kobayashi J, et al. Homologous recombination repair is regulated by domains at the N- and C-terminus of NBS1 and is dissociated with ATM functions. Oncogene 2007; 26: 6002-9.

43. Jongmans W, Vuillaume M, Chrzanowska K, Smeets D, Sperling K, Hall J. Nijmegen breakage syndrome cells fail to induce the p53-mediated DNA damage response following exposure to ionizing radiation. Mol Cell Biol 1997; 17: 5016-22.

44. Kanka C, Brozek I, Skalska B, Siemiatkowska A, Limon J. Germline NBS1 mutations in families with aggregation of Breast and/or ovarian cancer from north-east Poland. Anticancer Res 2007; 27: 3015–8.

45. Bogdanova N, Schürmann P, Waltes R, Feshchenko S, Zalutsky IV, Bremer M, et al. NBS1 variant I171V and breast cancer risk. Breast Cancer Res Treat 2008; 112: 75–9.

46. Taylor GM, O'Brien HP, Greaves MF, Ravetto PF, Eden OB. Mutations in the Nijmegen breakage syndrome gene (NBS1) in childhood acute lymphoblastic leukemia. Cancer Res 2003; 63: 6563–4.

Table 1. Association of *NBS1* variation with breast cancer in Japanese

SNP	Allele	Groups	Case			RAF	P[b]	OR[c] (95% C.I.)
Gene	1/2[a]		11	12	22			
rs61754966	G/A	Breast	0	23	1501	0.0075	0.0048	3.19 (1.36-7.44)
NBS1		Control	0	7	1455	0.0024		

I analyzed 1,524 breast cancers and 1,462 controls. [a]Allele 1; risk allele, Allele 2; non risk allele. P[b] value and Odd ratio (OR[c]) were calculated in a dominant model (11+12 vs 22).

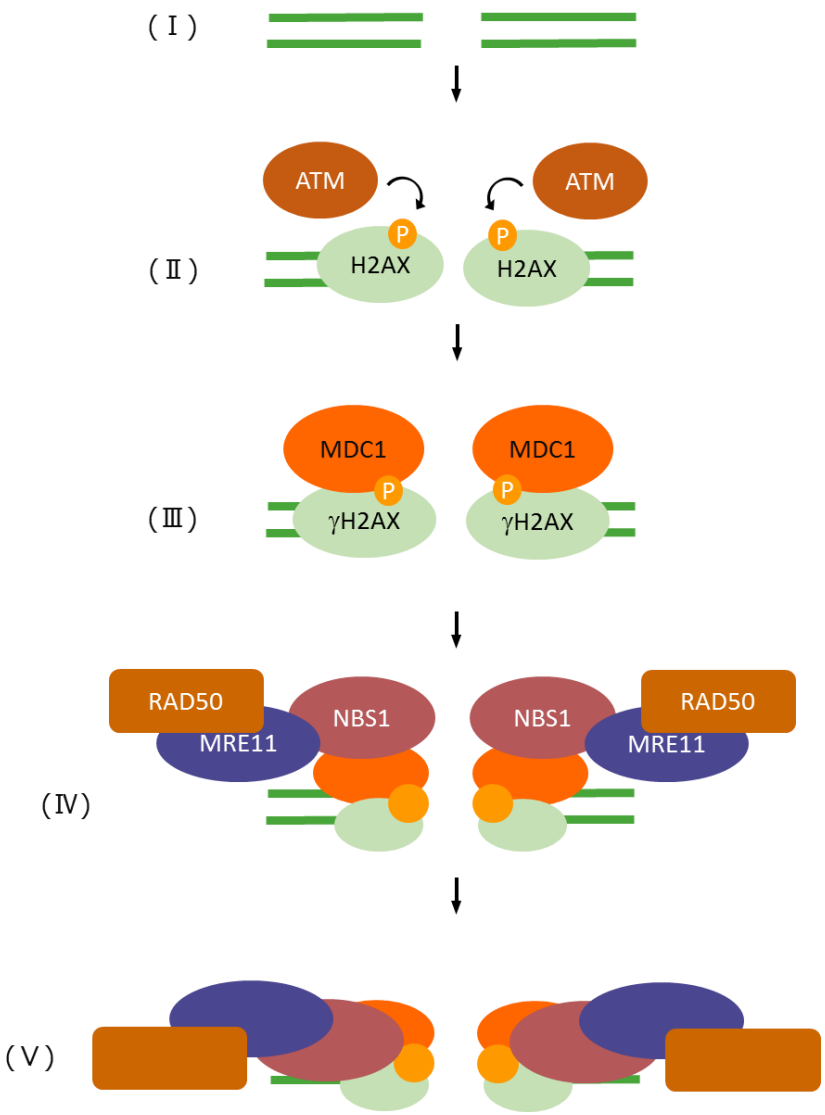

Fig.1 Early step of HR repair pathway

(Ⅰ) DNA Double Strand Breaks (DSB) on genomic DNAs. (Ⅱ) ATM accumulates to the DSB sites and phosphorylates H2AX (γH2AX). (Ⅲ) γH2AX recruits MDC1 to the DSB sites. (Ⅳ) MDC1 binds NBS1 and recruits MRN complex to the DSB sites. (Ⅴ) The MRN complex initiates resection of DSB ends.

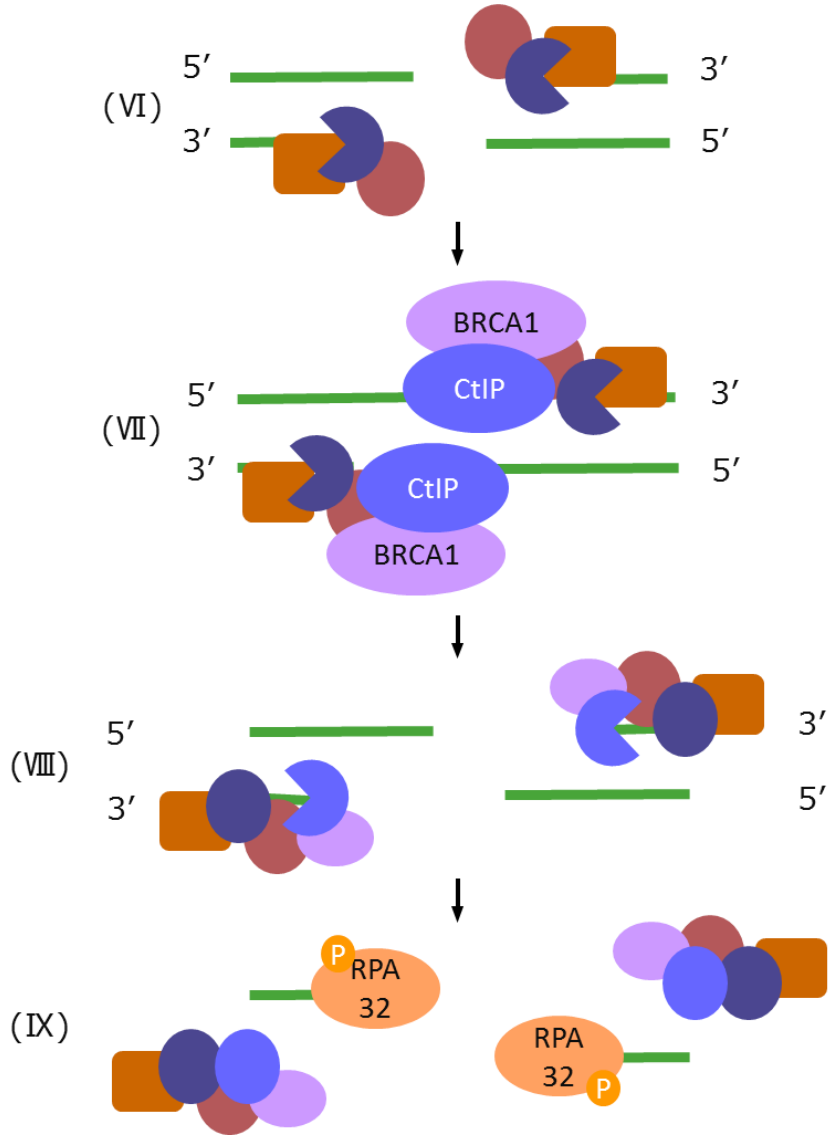

Fig. 2 The latter step of HR repair pathway

(Ⅵ) The MRN complex creates short single-stranded 3'-overhangs. (Ⅶ) The MRN complex recruits CtIP and BRCA1 to the DSB sites. (Ⅷ) CtIP creates long single-stranded 3'-overhangs. (Ⅸ) The MRN complex recruits RPA containing phosphorylated RPA32 to single-stranded 3'-overhangs.

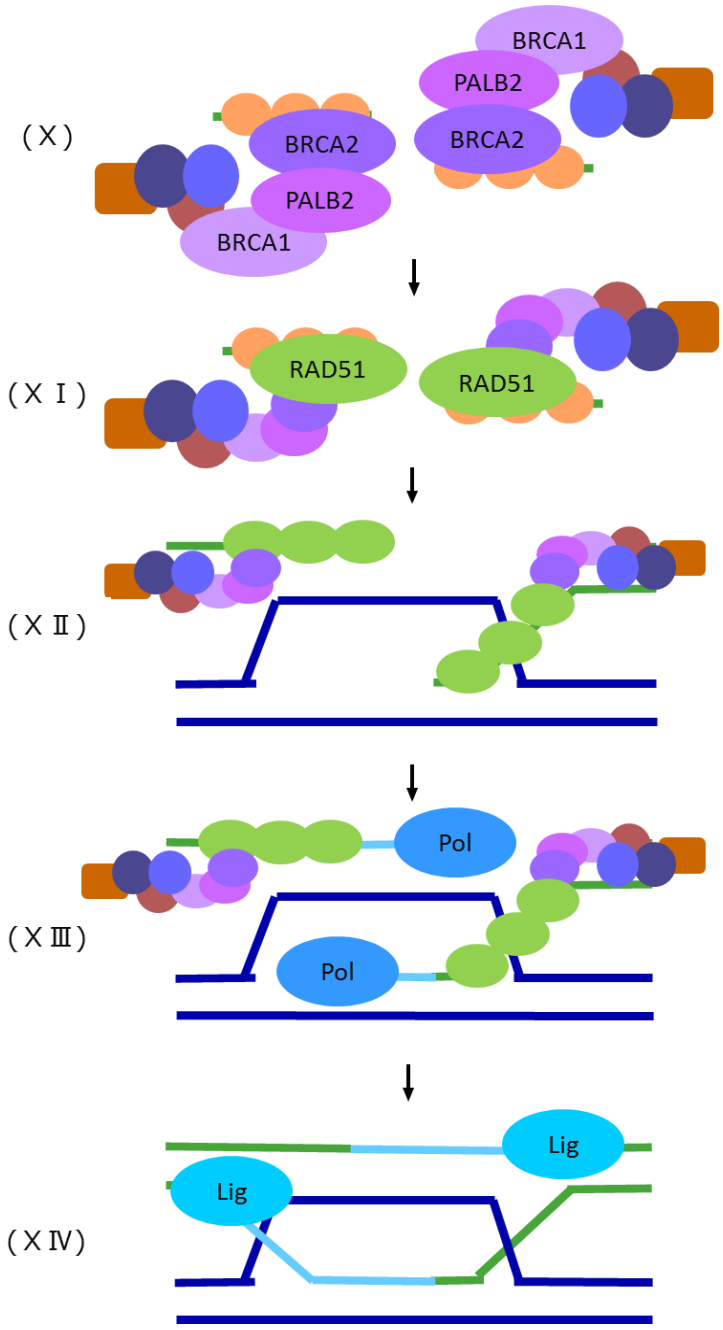

Fig. 3 The last step of HR repair pathway

(X) BRCA1 recruits BRCA2 to 3'-ssDNA through PALB2. (XⅠ) BRCA2 recruits RAD51 to 3'-ssDNA coated with RPA. (XⅡ) 3'-ssDNA invades complemental DNA strands with the strand exchange ability of RAD51. (XⅢ) DNA polymerase synthesizes new DNA strands. (XⅣ) DNA ligase attaches the new DNA ends to the DNA strand injured with DSB.

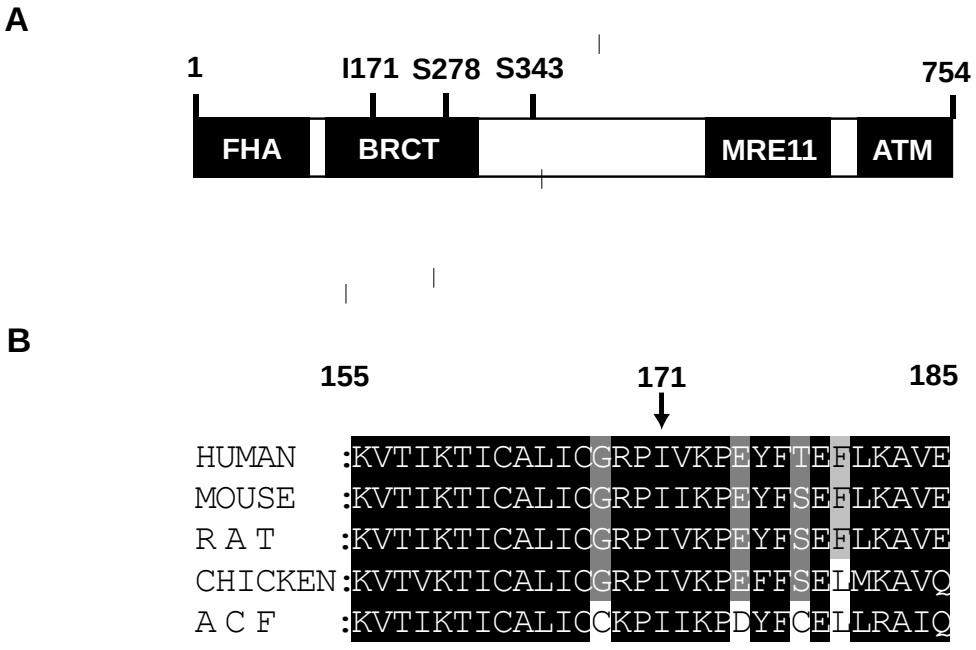

Fig. 4 The polymorphic variant of *NBS1*-I171V is located in the BRCT domain.

The structure of human NBS1 and the sequence alignment of the *NBS1*-I171V polymorphic variant region of NBS1. A, NBS1 consists of functional regions: forkhead-associated (FHA) and BRCT (BRCA1 C-terminus) domains at the N-terminus, MRE11 and ATM interacting motifs at the C-terminus and contain two phosphorylation sites (S278, S343) by ATM / ATR. B, Modified sequence alignment of the *NBS1*-I171V polymorphic variant region of various NBS1 from human, mouse, rat, chicken and ACF (African clawed frog, Xenopus laevis).

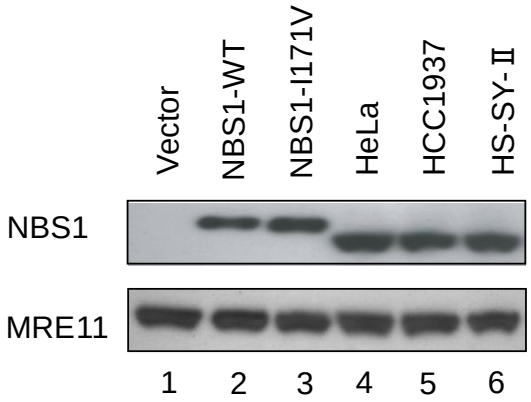

Fig. 5 Expression levels of NBS1 in the cells.

Expression vectors containing 3xFlag-His-HA -NBS1-WT cDNA, -NBS1-I171V cDNA, or no cDNA were stably transfected into GM07166VA7 cells. A, Expression levels of NBS1 in GM07166VA7 cells expressing NBS1-WT (WT), NBS-1I171 (I171V), the vector (vector), in HeLa cells, in HCC1937 cells and in HS-SY-II cells. Extracts from the cells were analyzed with antibodies directed against NBS1 or MRE11.

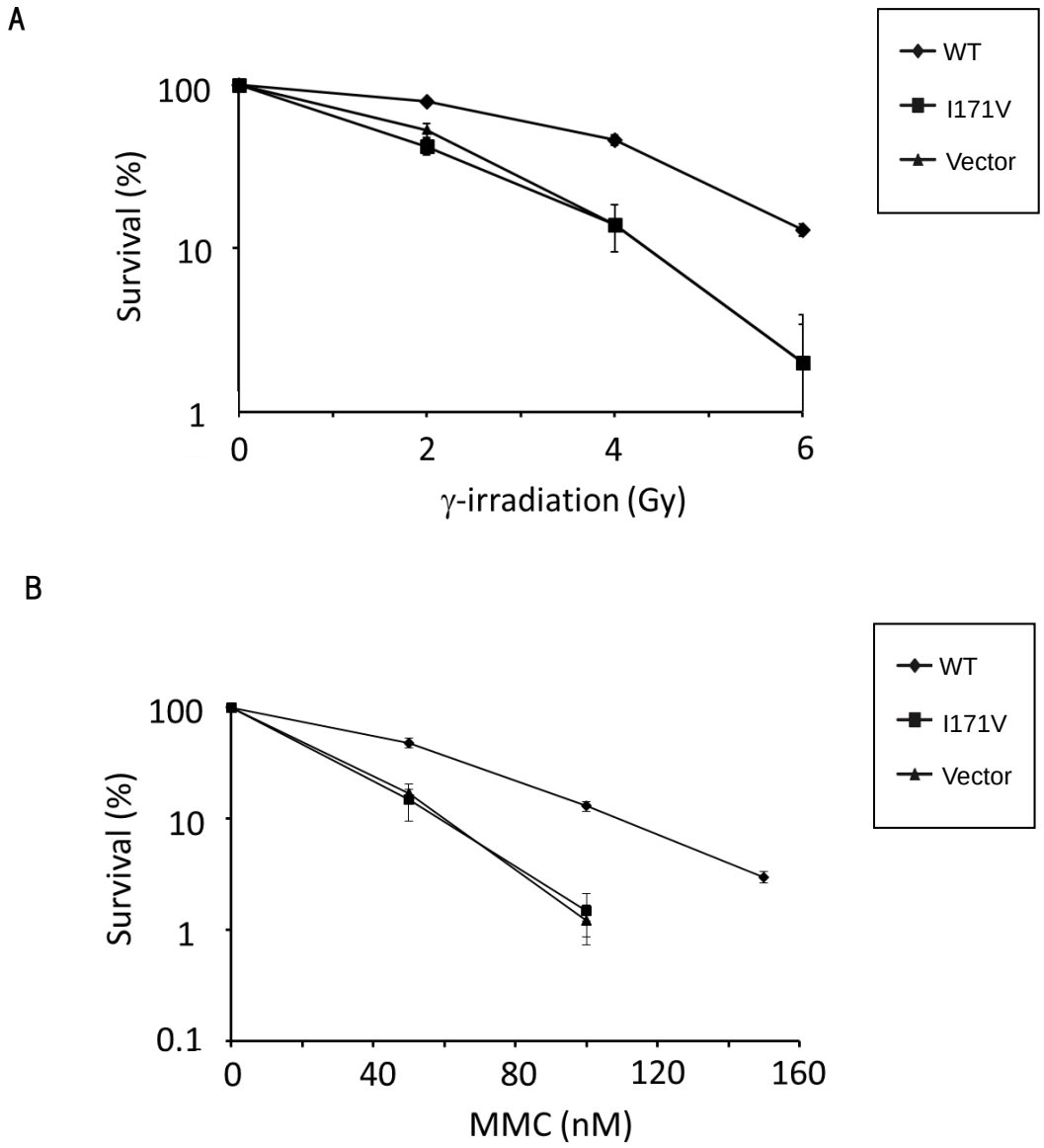

Fig. 6 The colony formation activity of the cells after exposure to γ-irradiation and MMC.

The survival of the GM07166VA7 cell lines expressing NBS1-WT (WT), NBS1-I171V (I171V) or the vector (vector) were analyzed by using a colony formation assay after exposure to 0, 2, 4 or 6 Gy of IR or 0, 50, 100 or 150 nmol/L of MMC. The data shown are the mean ± SEM (n = 3).

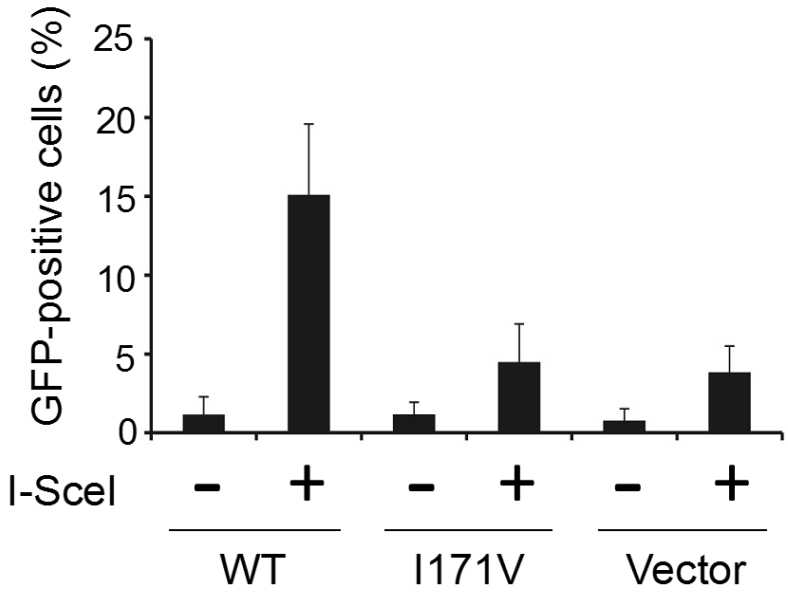

Fig. 7 The frequency of HR repair after the expression of I-SceI.

HR repair activity in the GM07166VA7 cell lines expressing NBS1-WT (WT), NBS1-I171V (I171V) or the vector (vector) was measured with the DR-GFP assay. The data shown are the mean ± SEM (n = 3).

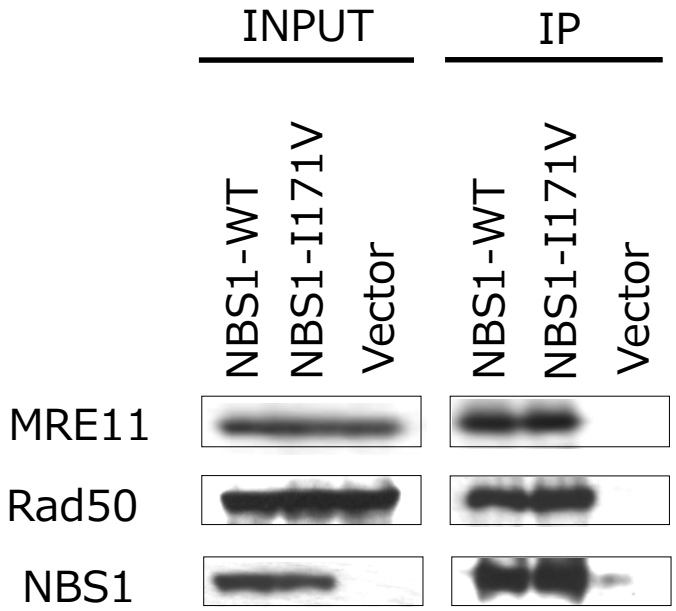

Fig. 8 Protein complex formation analysis of NBS1, MRE11 and RAD50.

Expression vectors containing 3xFlag-His-HA -NBS1-WT cDNA, -NBS1-I171V cDNA, or no cDNA (vector) were stably transfected into GM07166VA7 cells. Extracts from the cell lines were immunoprecipitated (IP) with anti-Flag antibody and then incubated with antibodies directed against MRE11, RAD50 or NBS1.

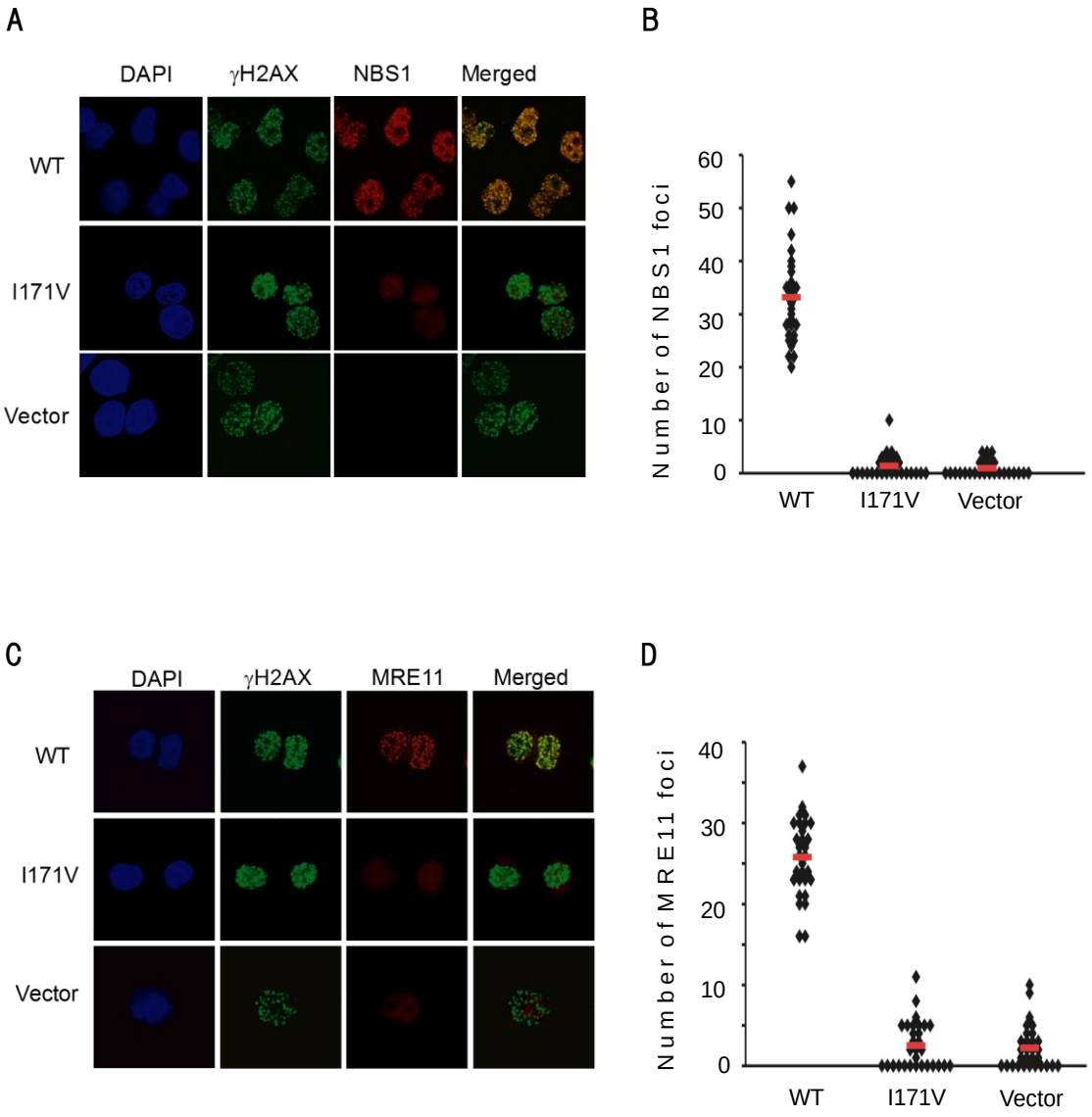

Fig. 9 Focus formation of NBS1, MRE11 and γH2AX in the cells.

A, C, Focus formation of NBS1, MRE11 and γH2AX. The GM07166VA7 cells expressing NBS1-WT (WT), NBS1-I171V (I171V) and the vector (vector) were irradiated with 10 Gy of IR. After 4 hours, the cells were incubated with antibodies directed against NBS1, γH2AX or MRE11, and then stained with DAPI. B, D, Scatter plots of NBS1 or MRE11 focus counts per cell in Fig. 9A or Fig. 9C are shown (n = 30). The red bars represent median.

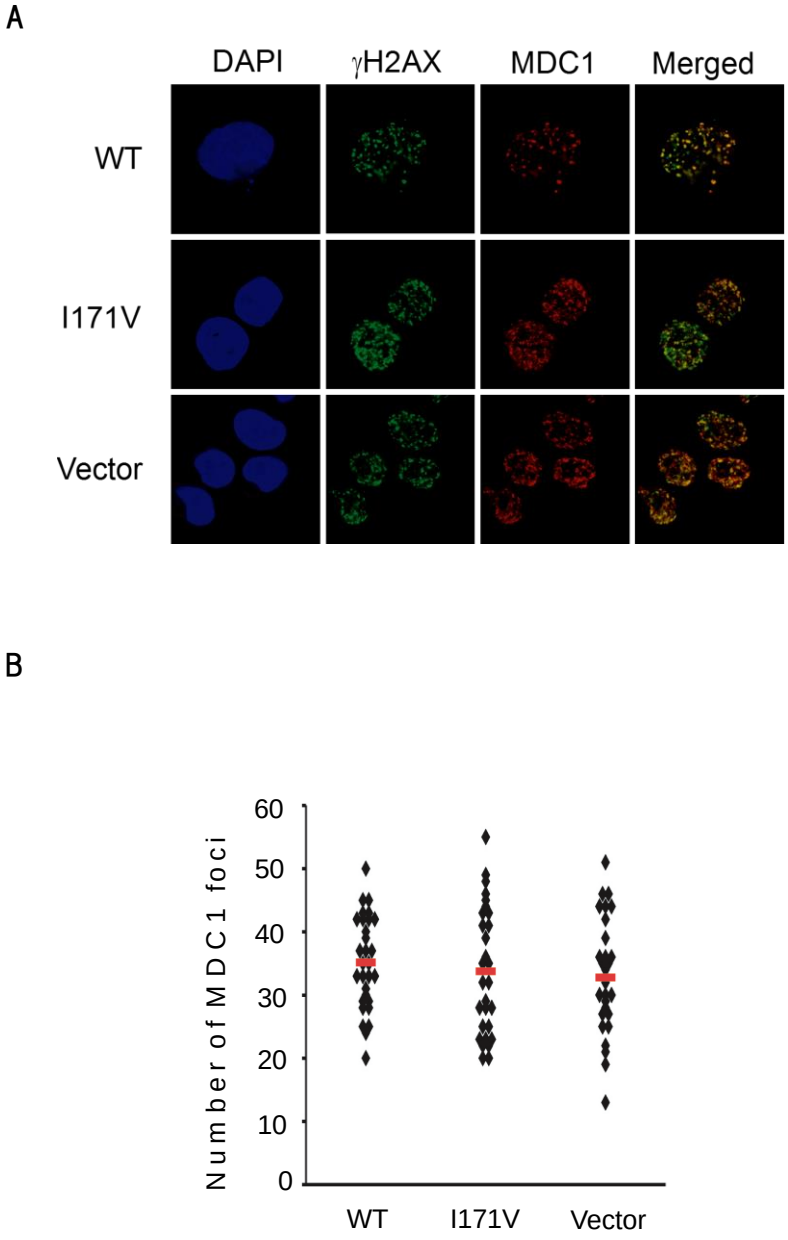

Fig. 10 Focus formation of γH2AX and MDC1 in the cells.

A, Focus formation of γH2AX and MDC1. The GM07166VA7 cells expressing NBS1-WT (WT), NBS1-I171V (I171V) and the vector (vector) were irradiated with 10 Gy of IR. After 4 hours, the cells were incubated with antibodies directed against γH2AX, MDC1, and then stained with DAPI. B, Scatter plots of MDC1 focus counts per cell in Fig. 10A are shown (n = 30). The red bars represent median.

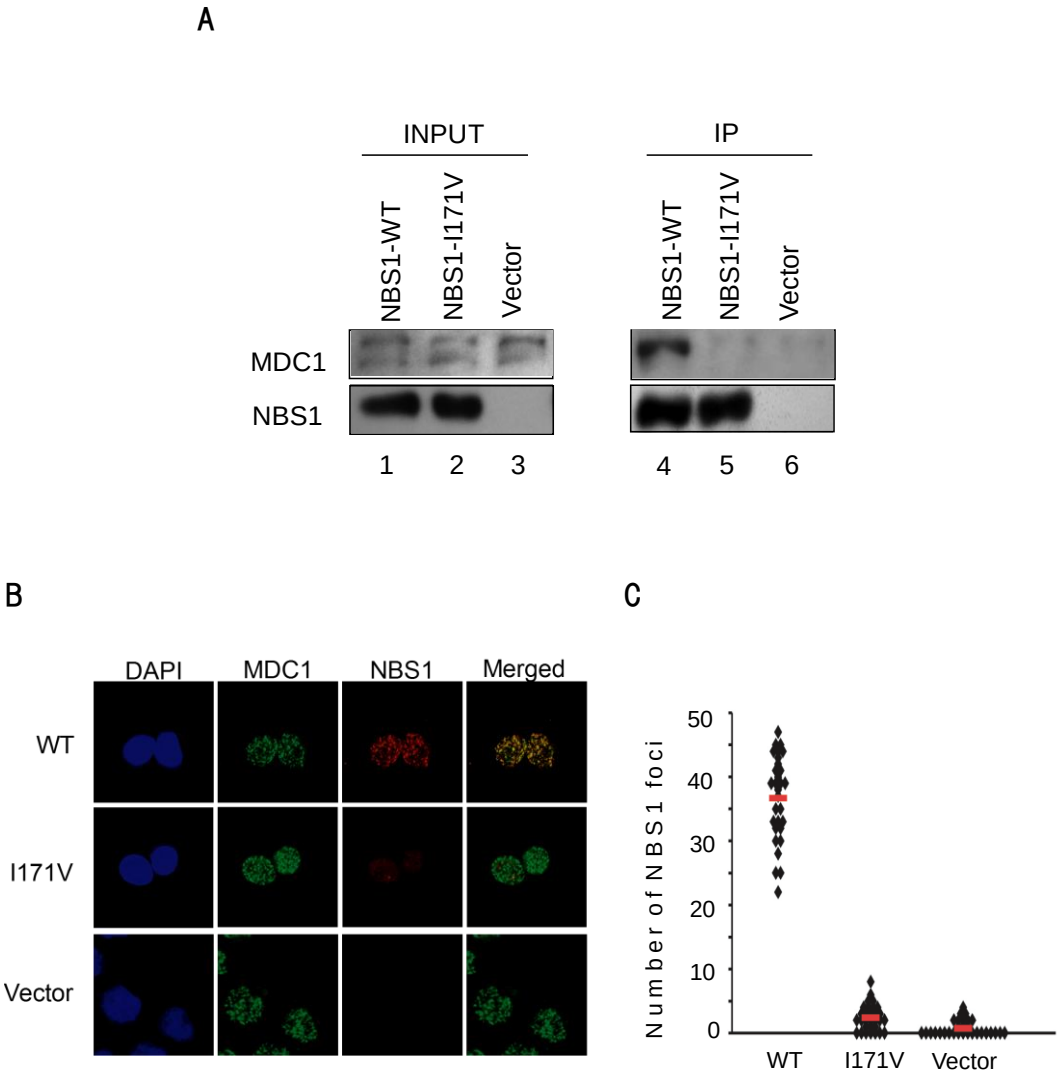

Fig. 11 Interaction analysis and focus formation of MDC1 and NBS1.

A, The GM07166VA7 cells expressing NBS1-WT, NBS1-I171V and the vector were irradiated with 10 Gy of IR. After 4 hours, whole cell lysates were prepared. The cell lysates were immunoprecipitated (IP) with anti-Flag antibody and then incubated with antibodies directed against MDC1 or NBS1.B, Focus formation of MDC1 and NBS1. The GM07166VA7 cells expressing NBS1-WT (WT), NBS1-I171V (I171V) and the vector (vector) were irradiated with 10 Gy of IR. After 4 hours, the cells were incubated with antibodies directed against MDC1 or NBS1, and then stained with DAPI. C, Scatter plots of NBS1 focus counts per cell in Fig. 11B are shown (n = 30). The red bars represent median.

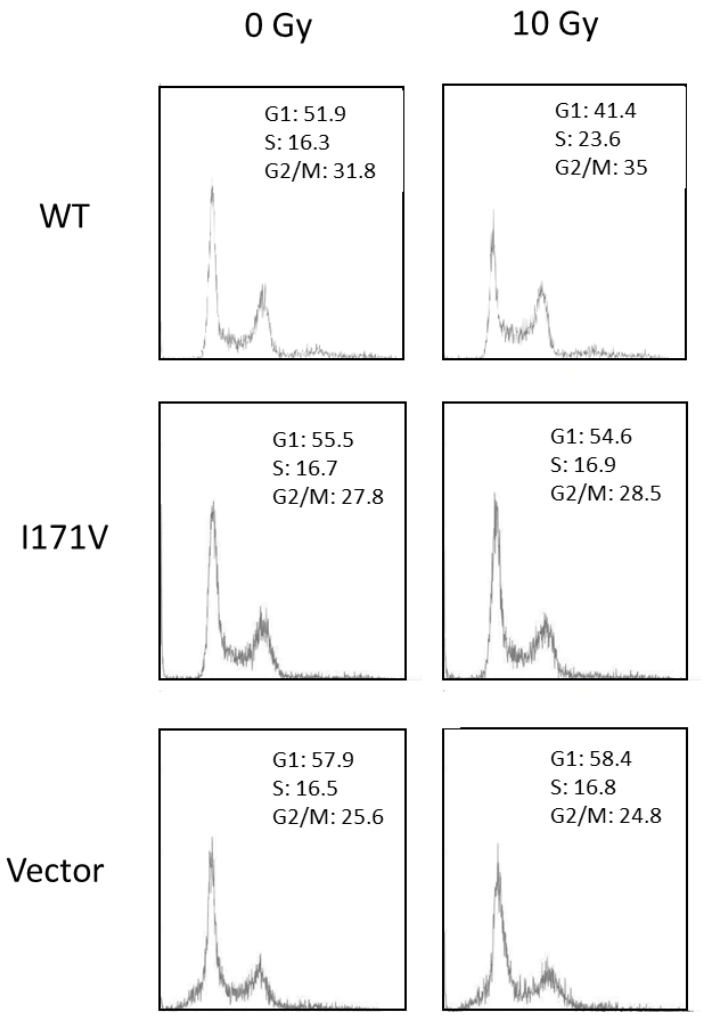

Fig. 12 The cells expressing an NBS1-I171V polymorphic variant doesn't stop the cell cycle after the γ-irradiation.

The cell lines expressing NBS1-WT (WT), NBS1-I171V (I171V), or the vector (vector) were irradiated with 10 Gy of IR. After 6 hours, the proportion of cells in the G1, S, and G2/M phases of the cell cycle were analyzed using a flow cytometer EC800 (Sony Biotechnology) and EC800 software.

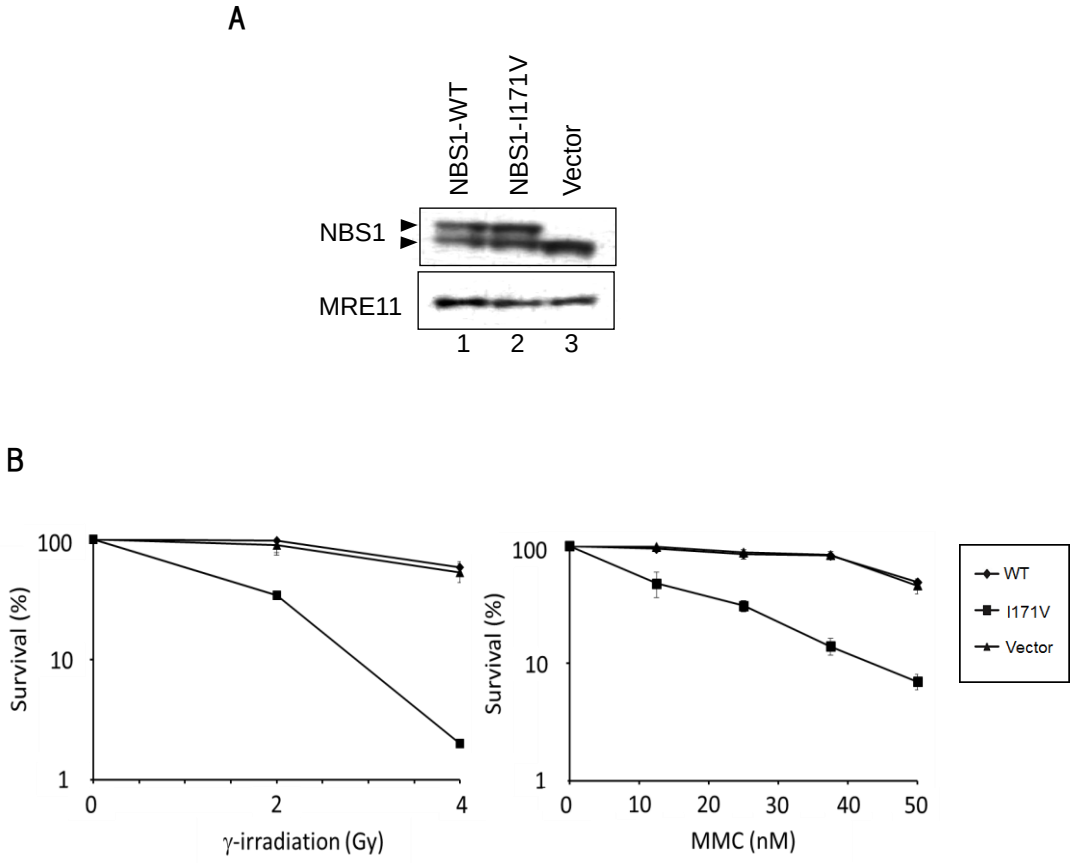

Fig. 13 The colony formation activity of the cell lines expressing NBS1-WT and I171V after exposure to γ-irradiation and MMC.

Expression vectors containing 3xFlag-His-HA-NBS1-WT cDNA, -NBS1-I171V cDNA, or no cDNA were stably transfected into HeLa cells. A, The expression levels of NBS1 in the cell extracts were analyzed with antibodies directed against NBS1. The upper *arrowhead* indicates exogenous NBS1 and the lower *arrowhead* indicates endogenous NBS1. B, The survival of the cell lines expressing NBS1-WT (WT), NBS1-I171V (I171V) or the vector (vector) was analyzed by using colony formation assays after exposure to 0, 2 or 4 Gy of IR or 0, 12.5, 25, 37.5 or 50n mol/L of MMC. The data shown are the mean ± SEM (n = 3).

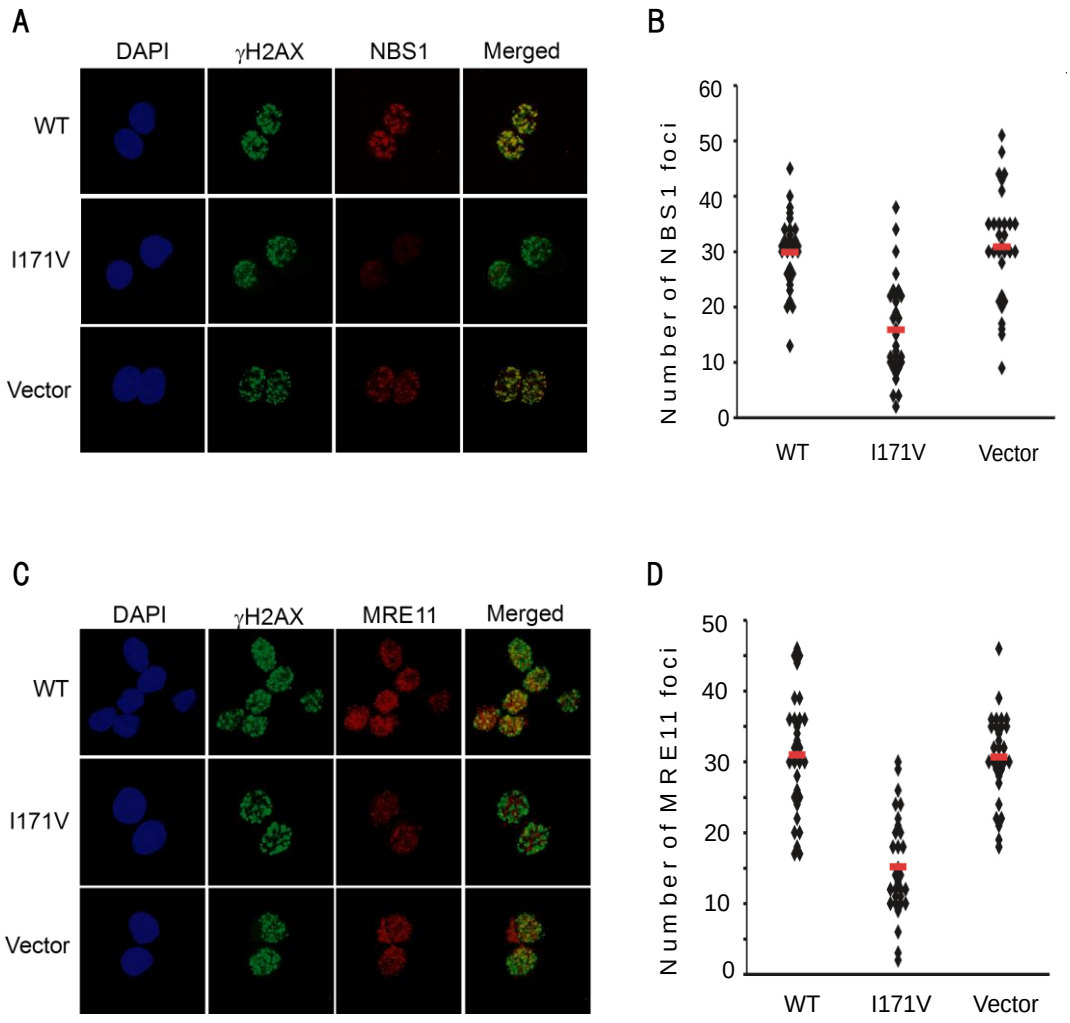

Fig. 14 Focus formation of NBS1 and MRE11 in HeLa cells expressing NBS1-I171V.

A, C, Focus formation of γH2AX, NBS1 and MRE11. The HeLa cells expressing NBS1-WT (WT), NBS1-I171V (I171V) and the vector (vector) were irradiated with 10 Gy of IR. After 4 hours, the cells were incubated with antibodies directed against γH2AX, NBS1 or MRE11, and then stained with DAPI. B, D, Scatter plots of NBS1 and MRE11 focus counts per cell in Supplementary Fig. 14A or 14C are shown (n = 30). The red bars represent median.

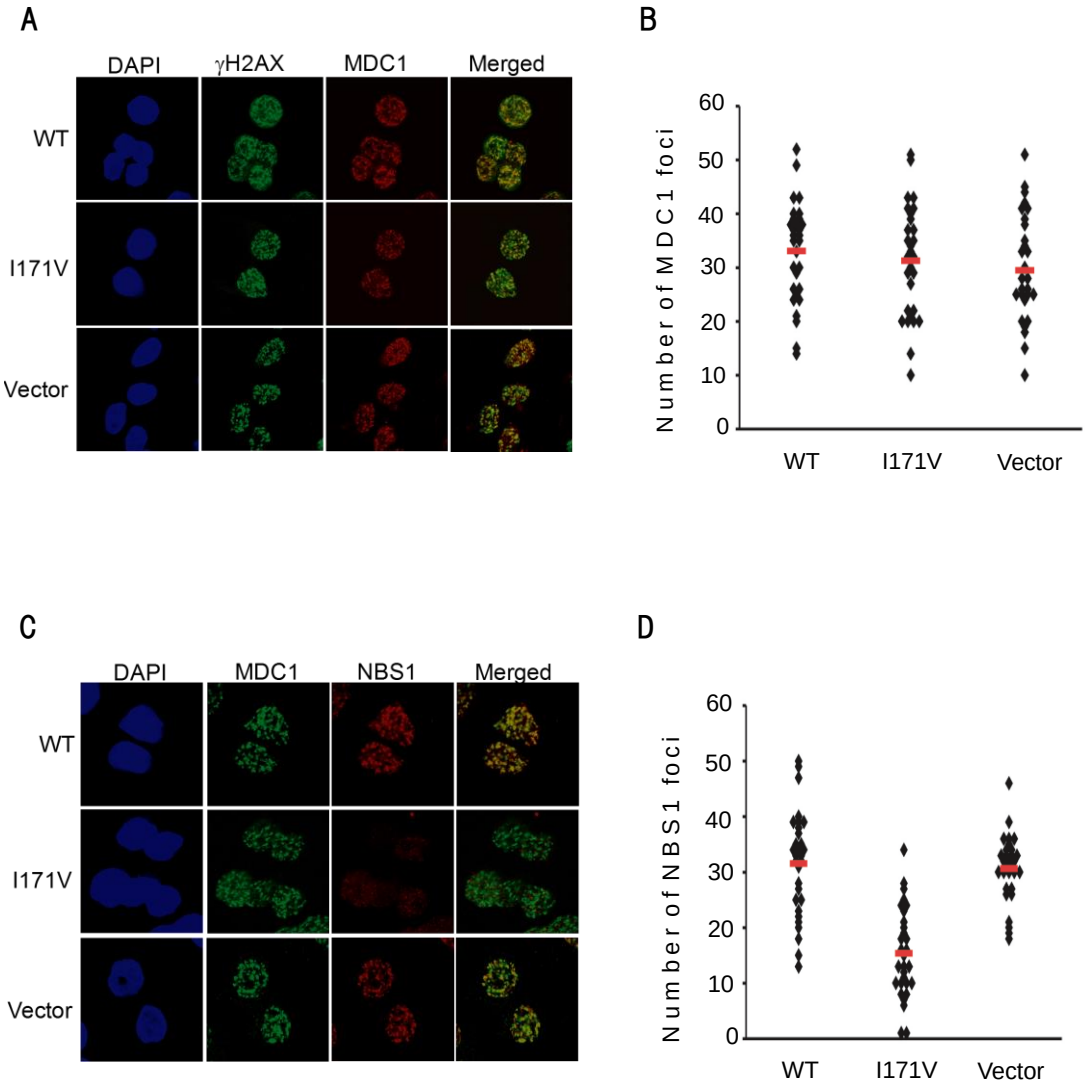

Fig. 15 Focus formation of MDC1 and NBS1 foci in HeLa cells expressing NBS1-I171V.

A, C, Focus formation of MDC1, γH2AX and NBS1. The HeLa cell lines expressing NBS1-WT (WT), NBS1-I171V (I171V) and the vector (vector) were irradiated with 10 Gy of IR. After 4 hours, the cells were incubated with antibodies directed against MDC1, γH2AX or NBS1, and then stained with DAPI. B, D, Scatter plots of NBS1 or MDC1 focus counts per cell in Supplementary Fig. 15A or 15C are shown (n = 30). The red bars represent median.

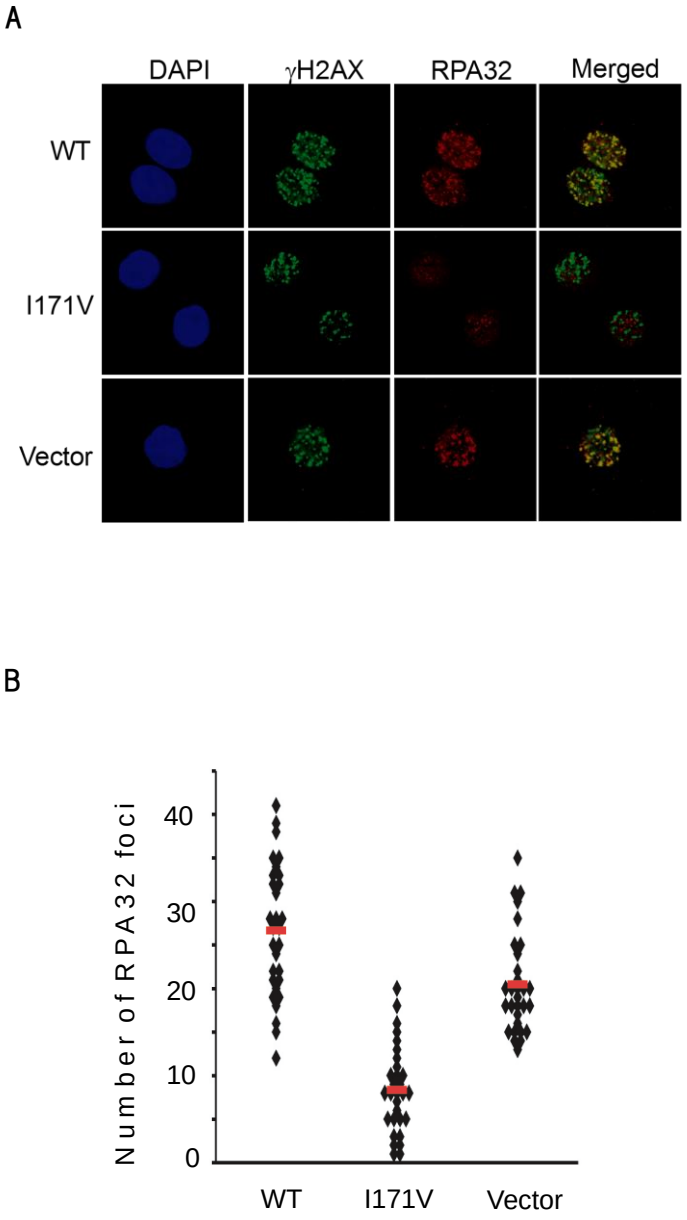

Fig. 16 Focus formation of RPA32 in HeLa cells expressing NBS1-I171V.

A, Focus formation of γH2AX and phosphorylated RPA32. The HeLa cells expressing NBS1-WT (WT), NBS1-I171V (I171V) and the vector (vector) were irradiated with 10 Gy of IR. After 4 hours, the cells were incubated with antibodies directed against γH2AX or RPA32, and then stained with DAPI. B, Scatter plots of RPA32 focus counts per cell in Fig. 16A are shown (n = 30). The red bars represent median.

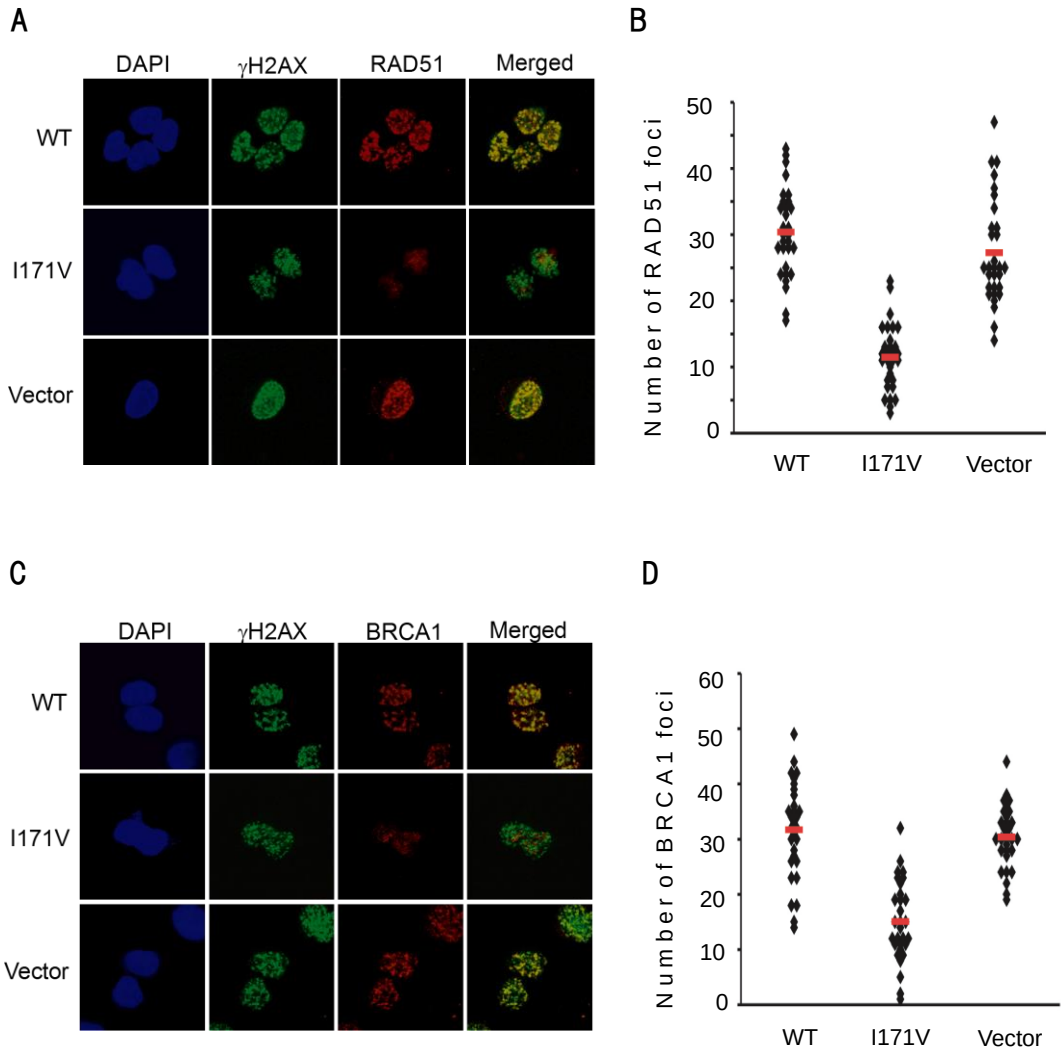

Fig. 17 Focus formation of BRCA1 and RAD51 in HeLa cells expressing NBS1-I171V.

A, C, Focus formation of γH2AX, RAD51 and BRCA1. The HeLa cells expressing NBS1-WT (WT), NBS1-I171V (I171V) and the vector (vector) were irradiated with 10 Gy of IR. After 4 hours, the cells were incubated with antibodies directed against γH2AX, RAD51 or BRCA1, and then stained with DAPI. B, D, Scatter plots of RAD51 or BRCA1 focus counts per cell in Fig. 17A or 17C are shown (n = 30). The red bars represent median.

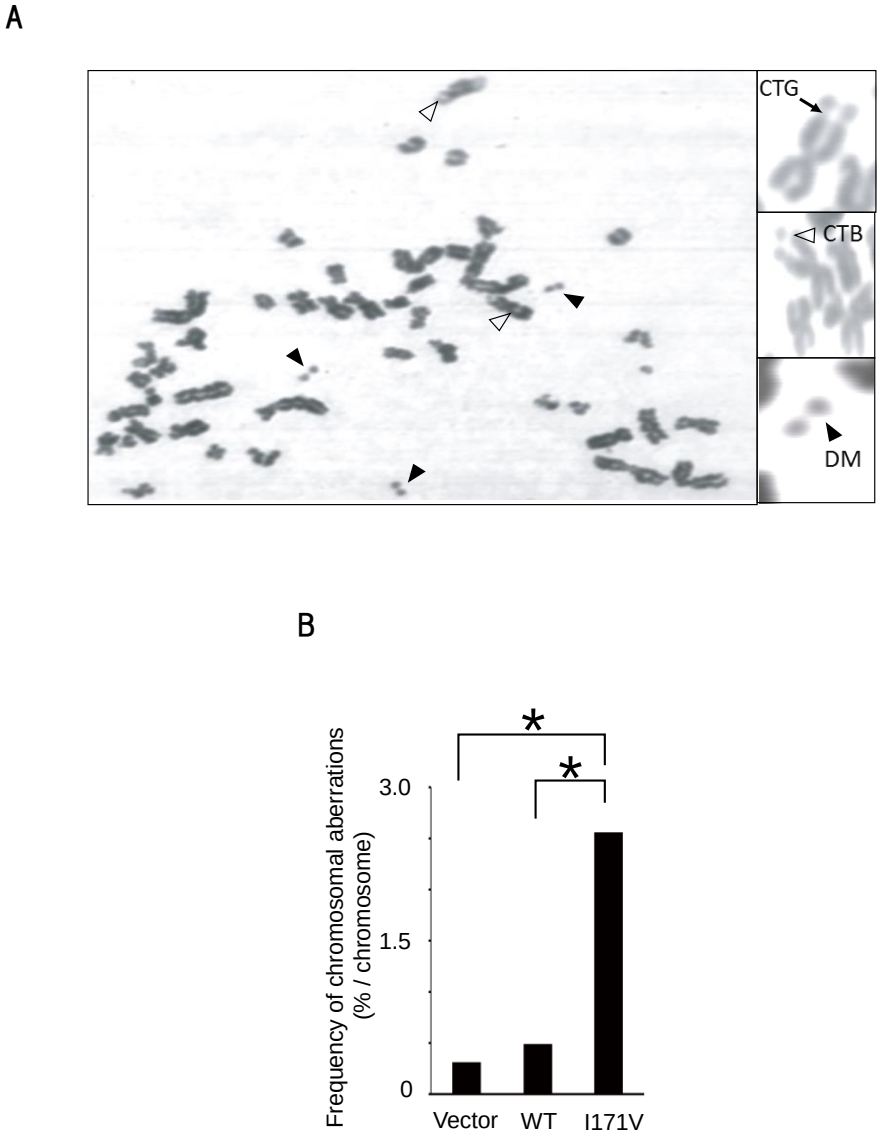

Fig. 18 The *NBS1*-I171V polymorphic variant elevates chromosomal instability.

A, representative metaphase spread of the HeLa cells expressing NBS1-I171V after exposure to 6 Gy of IR. Chromatid breaks (CTB, white *arrowheads*), double minutes (DM, black *arrowheads*), and chromatid gaps (CTG, *arrows*) are indicated. Noteworthy structural chromosomal aberrations are shown at higher magnification in the right panels: CTG (top panel), CTB (middle panel), and DM (bottom panel). B, Comparison of the frequencies of aberrations found in the cells used in Fig. 18A. *, $P < 0.005$.

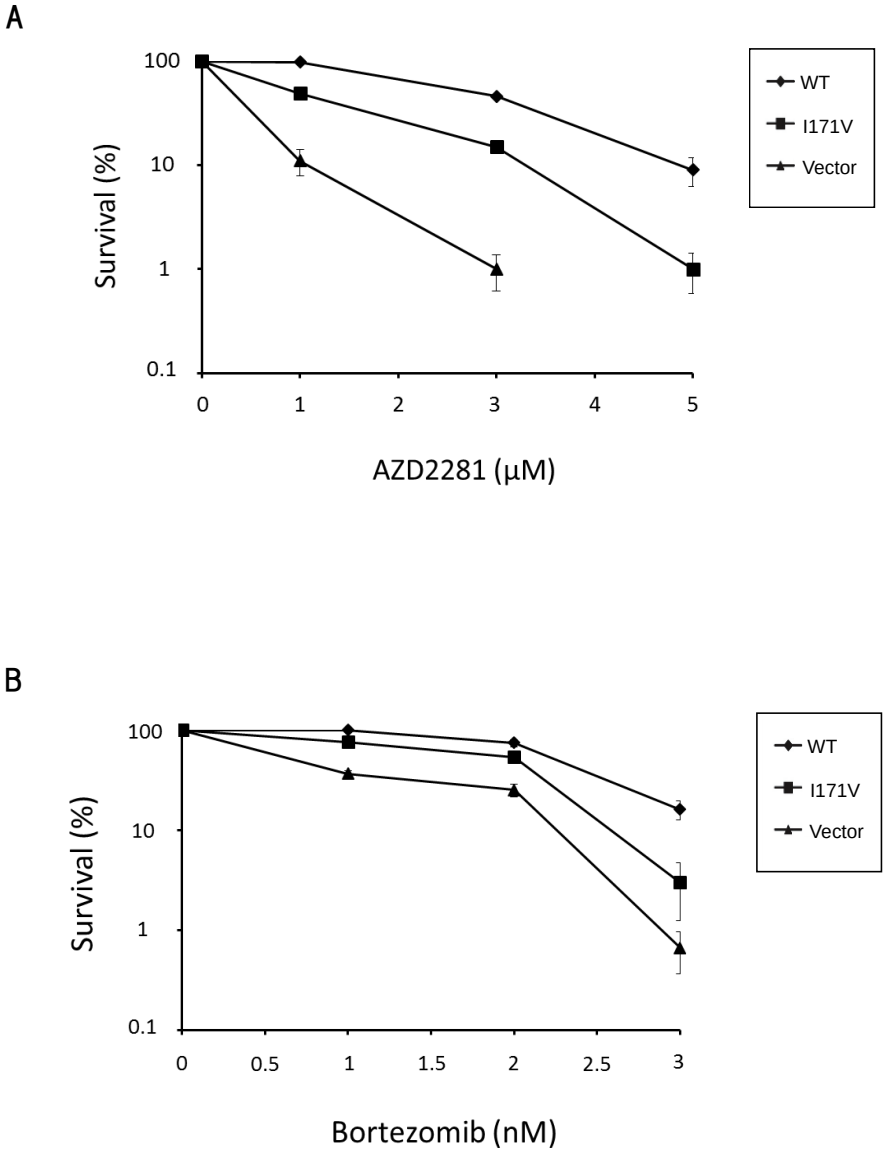

Fig. 19 The colony formation activity of the cells after exposure to AZD2281 and Bortezomib.

A, B, The survival of the GM07166VA7 cell lines expressing NBS1-WT (WT), NBS1-I171V (I171V) or the vector (vector) were analyzed by using a colony formation assay after treatment with 0, 1, 3 or 5 μM of AZD2281 or 0, 1, 2 or 3n mol/L of Bortezomib. The data shown are the mean ± SEM (n = 3).

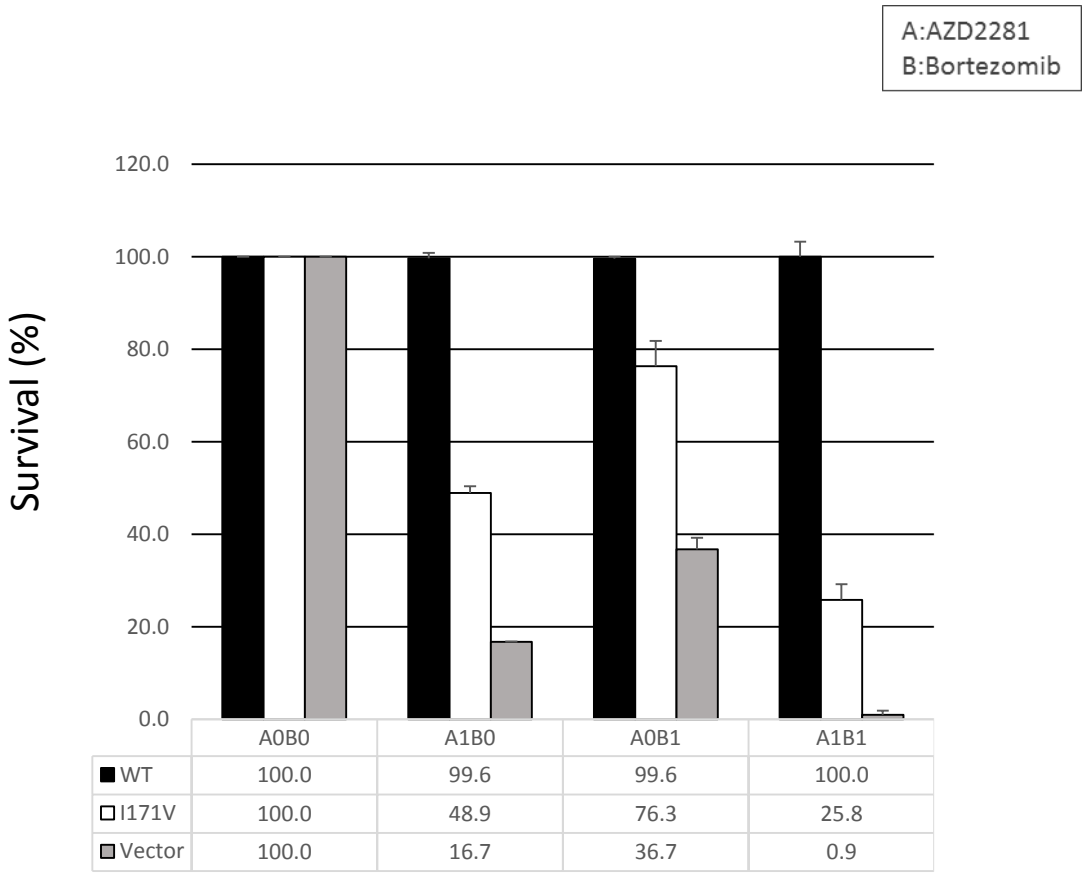

	A0B0	A1B0	A0B1	A1B1
WT	100.0	99.6	99.6	100.0
I171V	100.0	48.9	76.3	25.8
Vector	100.0	16.7	36.7	0.9

Fig. 20 The colony formation activity of the cells after the combination usage with AZD2281 and Bortezomib.

The survival of the GM07166VA7 cell lines expressing NBS1-WT (WT), NBS1-I171V (I171V) or the vector (vector) were analyzed by using a colony formation assay after treatment with 0 μmol/L of AZD2281 and 0 nmol/L of Bortezomib (A0B0), 1 μmol/L of AZD2281 and 0 nmol/L of Bortezomib (A1B0), 0 μmol/L of AZD2281 and 1 nmol/L of Bortezomib (A0B1) or 1 μmol/L of AZD2281 and 1 nmol/L of Bortezomib (A1B1).

The data shown are the mean ± SEM (n = 3).

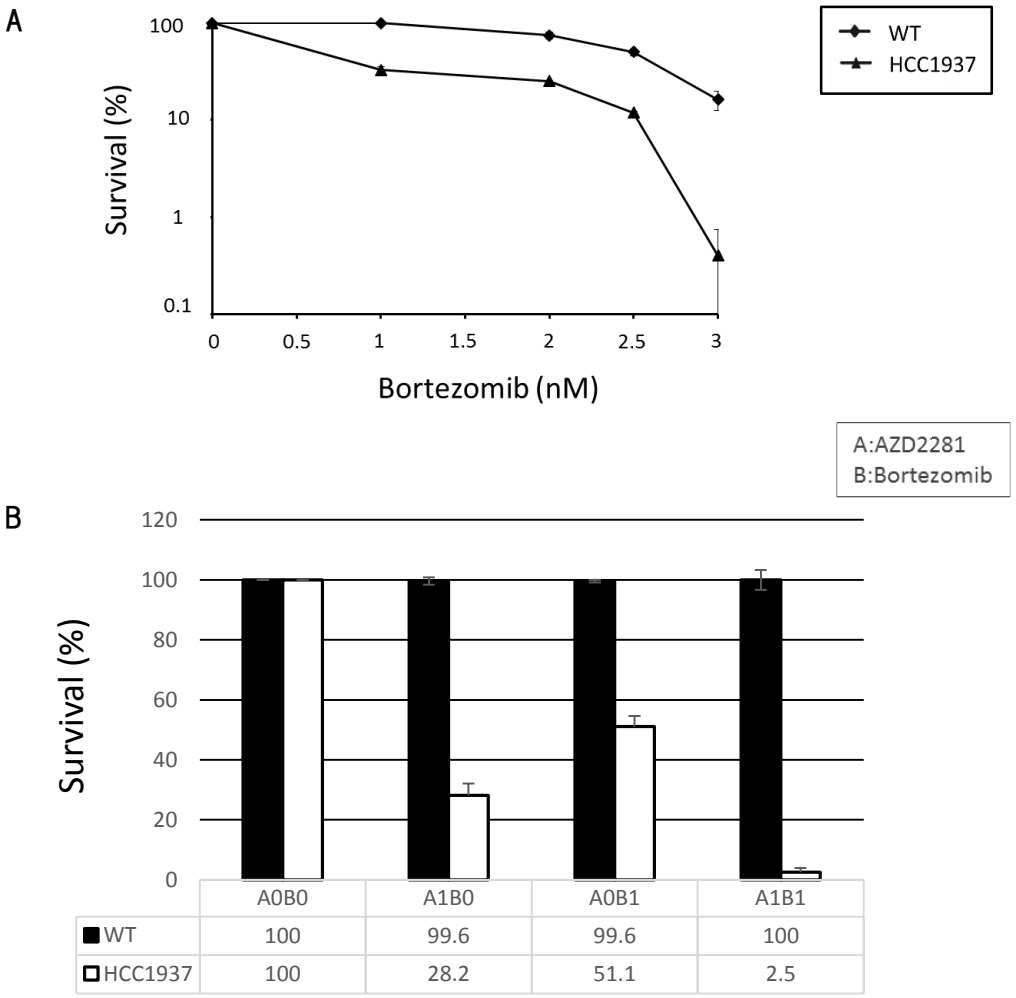

Fig. 21 The colony formation activity of HCC1937 cells after the combination usage with AZD2281 and Bortezomib.

A, The survival of the GM07166VA7 cell lines expressing NBS1-WT (WT) or HCC1937cells were analyzed by using a colony formation assay after treatment with 0, 1, 2, 2.5 or 3 nmol/L of Bortezomib. The data shown are the mean ± SEM (n = 3). B, The survival of the GM07166VA7 cell lines expressing NBS1-WT (WT) or HCC1937cells were analyzed by using a colony formation assay after treatment with 0 μmol/L of AZD2281 and 0 nmol/L of Bortezomib (A0B0), 1 μmol/L of AZD2281 and 0 nmol/L of Bortezomib (A1B0), 0 μmol/L of AZD2281 and 1 nmol/L of Bortezomib (A0B1) or 1 μmol/L of AZD2281 and 1 nmol/L of Bortezomib (A1B1). The data shown are the mean ± SEM (n = 3).

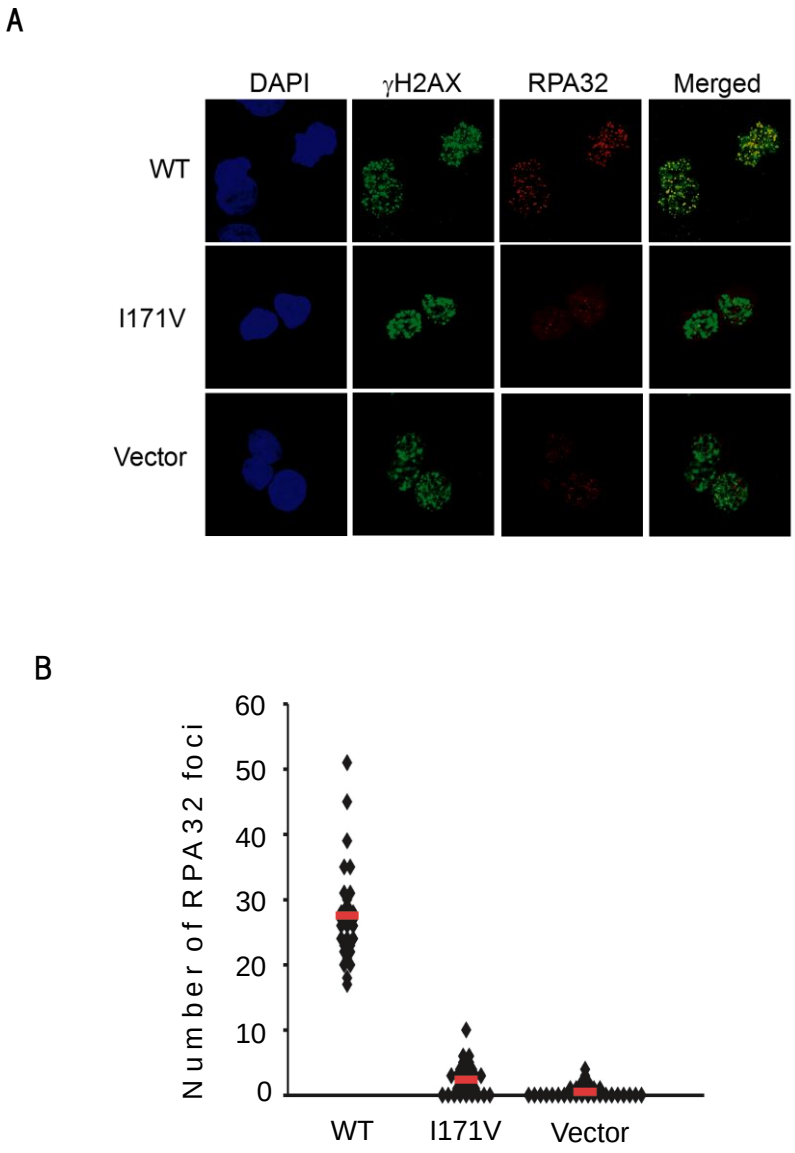

Fig 22 Focus formation of RPA32 in the cells.

A, Focus formation of γH2AX, phospho RPA32. The GM07166VA7 cells expressing NBS1-WT (WT), NBS1-I171V (I171V) and the vector (vector) were irradiated with 10 Gy of IR. After 4 hours, the cells were incubated with antibodies directed against γH2AX, phospho RPA32, and then stained with DAPI. B, Scatter plots of phospho RPA32 focus counts per cell in Fig. 22A are shown (n = 30). The red bars represent median.

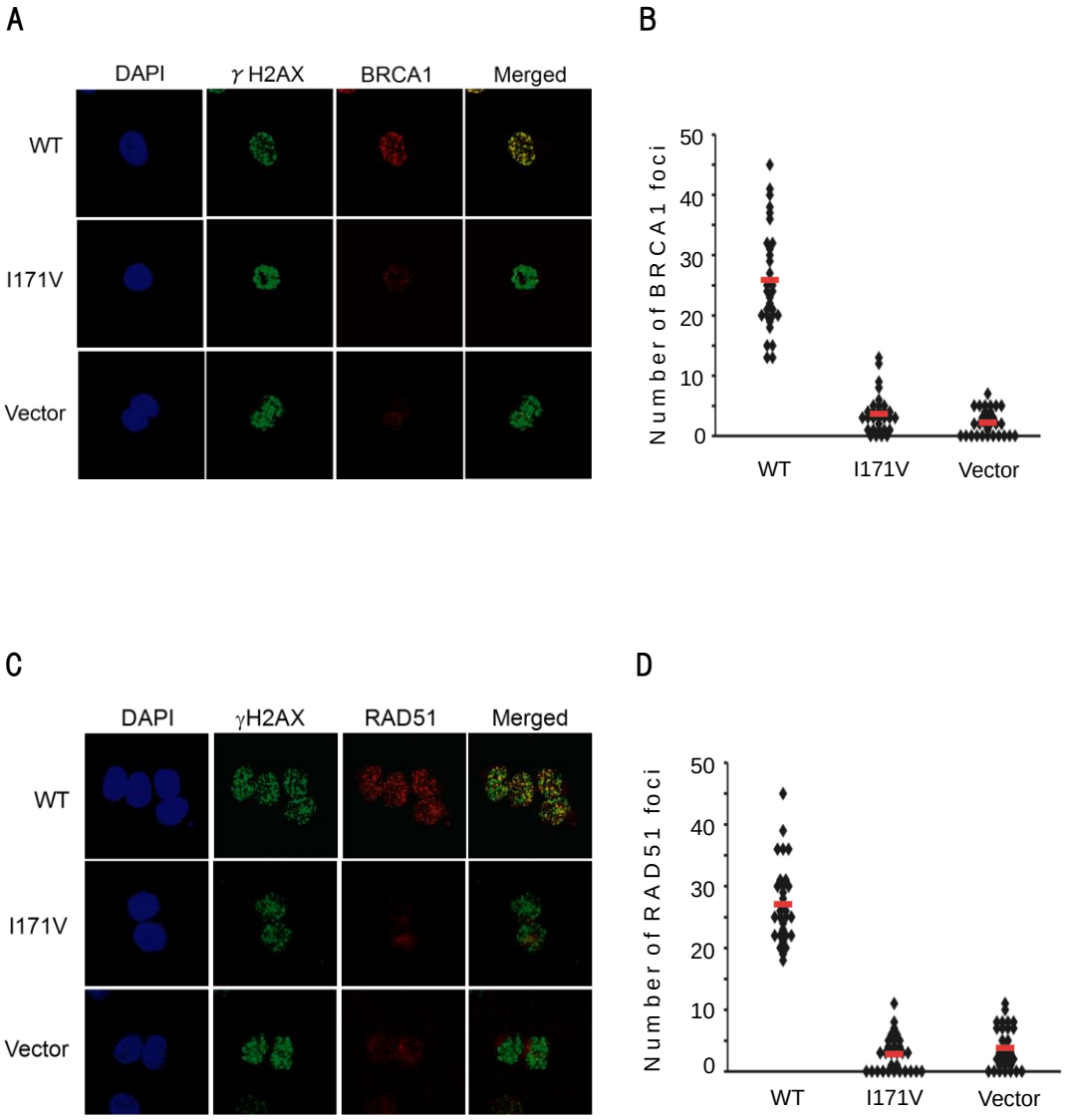

Fig 23 Focus formation of BRCA1 and RAD51 in the cells.

A, C, Focus formation of γH2AX, phospho BRCA1 and RAD51. The GM07166VA7 cells expressing NBS1-WT (WT), NBS1-I171V (I171V) and the vector (vector) were irradiated with 10 Gy of IR. After 4 hours, the cells were incubated with antibodies directed against γH2AX, phosphorylated BRCA1 or RAD51, and then stained with DAPI. B, D, Scatter plots of phospho BRCA1 or RAD51 focus counts per cell in Fig. 23A or Fig. 23C are shown (n = 30). The red bars represent median.

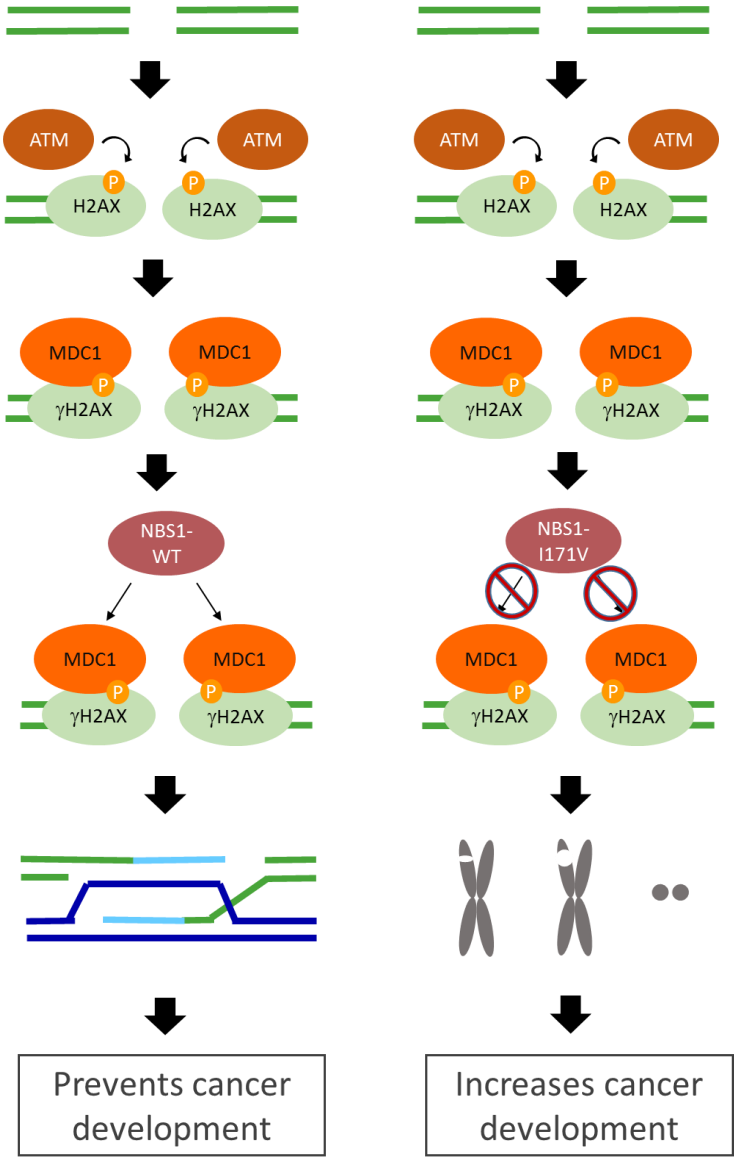

Fig. 24 The *NBS1*-I171V polymorphic variant could be associated with cancer development.

In normal cells ATM phosphorylates H2AX and MDC1 accumulates to γH2AX when DSBs were generated. Then NBS1-WT accumulates to MDC1 and promotes HR repair, and finally it could prevent cancer development. In the cells expressing NBS1-I171V ATM also phosphorylates H2AX and MDC1 accumulates to γH2AX when DSBs were generated. However NBS1-I171V reduces the interaction with MDC1 and does not accumulate DSB sites. From this loss of association with MDC1 the cells expressing NBS1-I171V reduces HR repair activity and increases chromosomal instability. Finally it could be associated with cancer development.